AMERICAN MUSEUM NOVITATES

Number 3952, 57 pp. June 3, 2020

The late middle Miocene Mae Moh Basin of northern Thailand: the richest Neogene assemblage of Carnivora from Southeast Asia and a paleobiogeographic analysis of Miocene Asian carnivorans

CAMILLE GROHÉ,[1] LOUIS DE BONIS,[1] YAOWALAK CHAIMANEE,[1] OLIVIER CHAVASSEAU,[1] MANA RUGBUMRUNG,[2] CHOTIMA YAMEE,[2] KANTAPON SURAPRASIT,[3] CORENTIN GIBERT,[1] JÉRÔME SURAULT,[1] CÉCILE BLONDEL,[1] AND JEAN-JACQUES JAEGER[1]

ABSTRACT

The late middle Miocene fossil-bearing lignite zones of the Mae Moh Basin, northern Thailand, have yielded a rich vertebrate fauna, including two species of Carnivora described thus far: the bunodont otter *Siamogale thailandica* (known from over a 100 specimens) and the large amphicyonid *Maemohcyon potisati*. Here we describe additional carnivoran material from Mae Moh comprising new remains of *Maemohcyon potisati* as well as remains of seven new carnivorans belonging to at least four families: a new species of *Siamogale* (*S. bounosa*), a new species of another otter (*Vishnuonyx maemohensis*), one representative of the genus *Pseudarctos* (a small amphicyonid), a new genus of Asian palm civet, *Siamictis*, one representative of another civet (cf. *Viverra* sp.), a new species of mongoose (*Leptoplesictis peignei*) and a Feliformia indet. This carnivoran assemblage constitutes one of the richest for the middle Miocene of eastern Asia and by far the richest for the Neogene of Southeast Asia.

[1] Laboratory Paleontology Evolution Paleoecosystems Paleoprimatology (PALEVOPRIM, UMR 7262 CNRS INEE), University of Poitiers, Poitiers, France.
[2] Department of Mineral Resources, Rama VI Road, Bangkok, Thailand.
[3] Department of Geology, Faculty of Science, Chulalongkorn University, Bangkok, Thailand.
and Department of Geosciences, Biogeology, University of Tübingen, Tübingen, Germany.

 ISSN 0003-0082

While the presence of new species indicates a certain degree of endemism for the Mae Moh Basin, paleobiogeographic cluster analyses conducted on carnivoran faunas from the middle and late Miocene of Asia indicates that a southern Asian biogeographic province, analogous to the current Oriental Realm, has existed since at least the middle Miocene. These results strengthen the observation that the Himalayan Mountains and Tibetan Plateau constitute significant physical barriers as well as an important climatic barrier (through the strengthening of monsoon systems) preventing north-south mammal dispersals in Asia since at least the middle Miocene.

INTRODUCTION

Continental Cenozoic basins of Thailand have yielded numerous vertebrate faunas. Northern Thailand comprises several fossiliferous intermontane basins of middle Miocene age. The main mammal-bearing localities are situated in the basins of Li, Mae Moh, Pong, and Chiang Muan (Koenigswald, 1959; Ginsburg et al., 1983; Ginsburg and Tassy, 1985; Tassy et al., 1992; Ducrocq et al., 1994, 1995; Mein and Ginsburg, 1997; Chaimanee et al., 2003; Peigné et al., 2006; Chaimanee et al., 2007, 2008; Chavasseau et al., 2009; Grohé et al., 2010; Chaimanee et al., 2011; Suraprasit et al., 2011; Grohé et al., 2013; Suraprasit et al., 2014, 2015), the latter having yielded the large-bodied hominoid *Khoratpithecus chiangmuanensis* (Chaimanee et al., 2003). In Southeast Asia, Miocene Carnivora are known from six species from northern Thailand: the amphicyonid cf. *Amphicyon* sp. from the early middle Miocene locality of Ban San Klang, Pong Basin (Ducrocq et al., 1994, 1995); the mustelid ?*Martes* sp. and the viverrid ?*Semigenetta* sp. from the early middle Miocene locality of Mae Long, Li Basin (Mein and Ginsburg, 1997); the mustelid *Siamogale thailandica* (Ginsburg et al., 1983; Grohé et al., 2010) and the amphicyonid *Maemohcyon potisati* (Peigné et al., 2006) from the late middle Miocene Mae Moh Basin; and the mustelid *Sivaonyx* cf. *gandakasensis* from the late middle Miocene of Ban Sa, Chiang Muan Basin (Grohé et al., 2013). In the middle Miocene of Asia, the most productive fossiliferous areas for Carnivora are the Halamagai Formation of Junggar Basin (Qi, 1989; Wang et al., 1998; Jiangzuo et al., 2018; Valenciano et al., 2019; Wang et al., 2020), the Tunggur Formation of Inner Mongolia (Colbert, 1939; Wang et al., 2003; Wang, 2004; Tseng et al., 2009) and the Chinji Formation of Pakistan (Pilgrim, 1932; Colbert, 1933; Pilbeam et al., 1979). We describe here new material of mustelids, amphicyonids, viverrids, and one herpestid from the late middle Miocene lignite zones of the Na Khaem Formation, Mae Moh Basin. This fauna substantially increases our knowledge of carnivoran evolution in the Miocene of southern Asia and provides new clues to improve the paleobiogeographic history of mammalian faunas from the middle Miocene of Asia.

Geological Setting

The Mae Moh coal mine is located in the Mae Moh district of the Lampang Province, northern Thailand (fig. 1). This intermontane basin is the largest open coal mine of Thailand and is intensively exploited by the EGAT (Electricity Generating Authority of Thailand) for

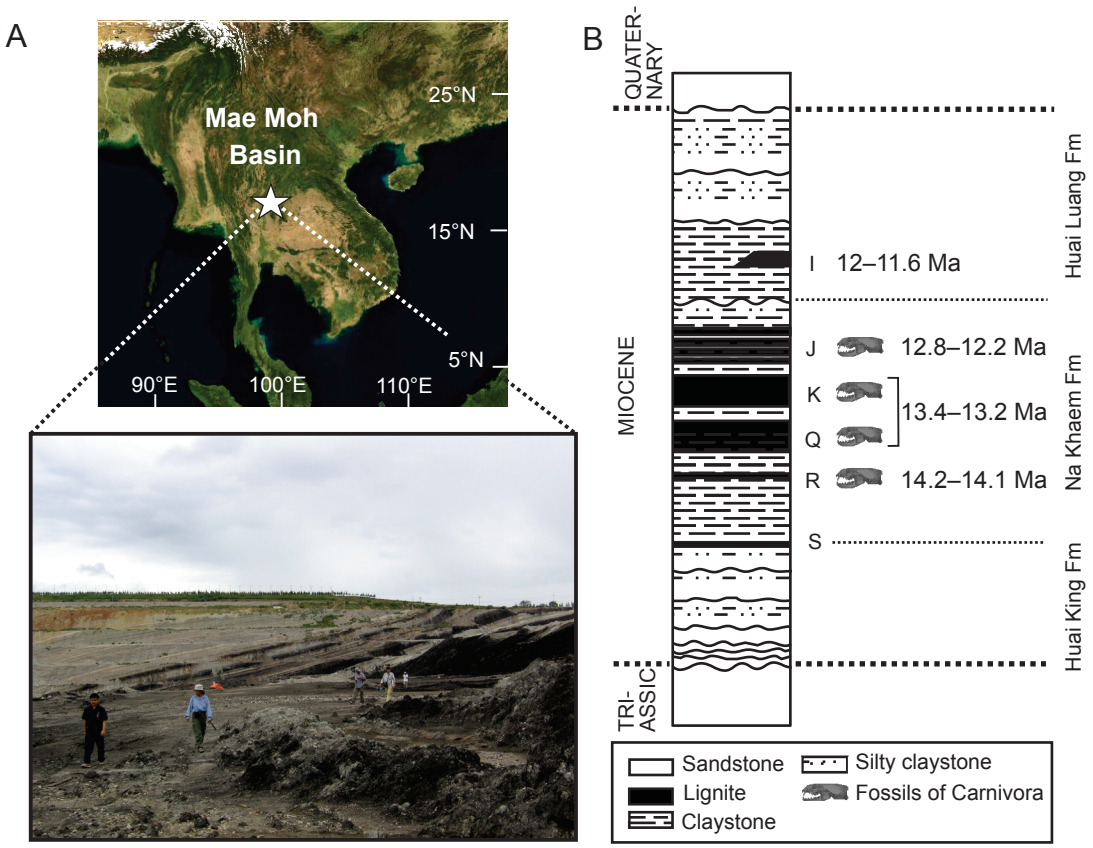

FIGURE 1. Mae Moh Basin, northern Thailand. **A,** Location of the basin and view of the southwest pit where the most fossiliferous lignite zones Q and K are found. Photo by O.C.; **B,** Lithostratigraphic sequence of the basin with Carnivora-bearing zones and paleomagnetical dates from Benammi et al. (2002) and Coster et al. (2010).

its mineral resources. The Miocene filling of the basin, known as the Mae Moh Group, is nearly 1000 meters thick and is composed of claystones, mudstones, siltstones, and sandstones alternating with lignite zones (named S, R, Q, K, J, and I from base to top; fig. 1). It is divided into three formations: the Huai King, Na Khaem, and Huai Luang Formations, in ascending order (Corsiri and Crouch, 1985). The Na Khaem Formation is 300 to 420 m thick and contains the main coal zones (R to J), in which fossils are abundant. The fauna includes fish, turtles, crocodiles, amphibians, and mammals (von Koenigswald, 1959; Ginsburg et al., 1983; Ginsburg and Tassy, 1985; Tassy et al., 1992; Ducrocq et al., 1994, 1995; Peigné et al., 2006; Chaimanee et al., 2007, 2008; Chavasseau et al., 2009; Grohé et al., 2010; Chaimanee et al., 2011; Suraprasit et al., 2011, 2014, 2015), but also invertebrate fossils such as gastropods and bivalves (Songtham et al., 2005). Plant remains such as fossil leaves, charophytes, and pollens are also part of the Mae Moh fossil record (e.g., Sepulchre et al., 2010). Palynological assemblages indicate the presence of a warm tropical forest, including among others freshwater swampy taxa, surrounded by a midlatitude deciduous forest. Along with mollus-

can assemblages, sedimentological studies suggest that the deposits of the Na Khaem Formation occurred in freshwater environments typical of ephemeral lakes or peat swamps. From 2004 to 2019, a Thai-French team (Department of Mineral Resources of Bangkok and University of Poitiers, France) has recovered Carnivora remains from the R, Q–K, and J lignite zones, dated by magnetostratigraphy to 14.2–14.1 Ma, 13.4–13.2 Ma and 12.8–12.2 Ma, respectively (Benammi et al., 2002; Coster et al., 2010; fig. 1).

Material and Methods

Most of the Thai material described in this study is stored at the Department of Mineral Resources of Bangkok (DMR), Thailand. Some specimens are stored at the Laboratoire Paléontologie Evolution Paléoécosystèmes Paléoprimatologie (PALEVOPRIM), University of Poitiers, France. All the fossil carnivorans come from the Q–K lignite zones (13.4–13.2 Ma), with the exception of one specimen of *Vishnuonyx maemohensis*, n. sp., recovered from the R lignite zone (14.2–14.1 Ma), and a skull of *Siamogale bounosa*, n. sp., recovered from the J lignite zone (12.8–12.2 Ma) (Benammi et al., 2002; Coster et al., 2010).

Institutional and Fossil Abbreviations

The following institutional and fossil abbreviations are used: **AD,** fossils from Arrisdrift, Geological Survey of Namibia; **AM,** American Museum of Natural History, New York; **ASK-VP,** Asa Koma Vertebrate Paleontology, Middle Awash, Ethiopia; **BAR,** fossils from Baringo District, Community Museums of Kenya; **BMNH,** Natural History Museum, London; **BSPG,** Bayerische Staatssammlung für Paläontologie und historische Geologie, Munich; **DPC,** Duke University Primate Center, Durham, NC; **ER,** fossils from East Rudolf (old name for Lake Turkana); **FLK,** Frida Leakey Korongo, Olduvai Gorge, Tanzania: **-N,** North; **-NN,** North-North; **FSL,** Faculté des Sciences de la Terre, Université Claude Bernard, Lyon, France: **VxC,** fossils from Vieux-Collonges (Rhône), France; **GAW-VP,** Gawto vertebrates, lower part of the Haradaso Member of the Sagantole Formation, Middle Awash, Ethiopia; **GSI,** Geological Survey of India, Calcutta; **GSP-Y,** Geological Survey of Pakistan, Quetta–Yale University, New Haven, CT; **GT,** fossils from Grillental, Sperrgebiet, Namibia; **HMN,** Hiwa Museum of Natural History, Hiwa Town, Hiba-Gun, Hiroshima Prefecture, Japan; **IVPP V,** Institute of Vertebrate Paleontology and Paleoanthropology, Beijing, vertebrate collection; **KE,** Kapchagay Geological Expedition, Ministry of Ecology and Natural Resources of the Kazakhstan Republic: **-Ask,** Askazansor; **KNM,** Kenya National Museums, Nairobi: **-BN,** Ngorora; **-FT,** Fort Ternan; **-LT,** Lothagam; **-MO,** Moruorot; **-RU,** Rusinga; **-LT,** Langetal, Sperrgebiet, Namibia; **MM,** fossils from Mae Moh, Thailand; **MNHN,** Muséum d'Histoire Naturelle de Paris: **-Ar,** Artenay (Loiret), France; **-L Gr,** La Grive-Saint-Alban (Isère), France; **-Sa,** Sansan (Gers), France; **NHMB,** Naturhistorisches Museum Basel, Switzerland: **-Ss,** Sansan, France; **NK,** fossils from Nkondo, Uganda National Museum, Kampala; **O** or **OMO,** fossils from Shungura Formation, Omo Group, Ethiopia; **PAK,** fossils from Dera Bugti, Pakistan; **PDYV,** "Pan Den Program" Yunnan

Vertebrate collection, Yunnan Institute of Culture Relics and Archaeology, Kunming, Yunnan Province, China; **SMNS,** Staatliches Museum für Naturkunde von Stuttgart, Germany; **TF,** Thai Fossils, Department of Mineral Resources, Bangkok, Thailand; **TM,** fossils from Toros-Menalla, Chad; **WIHG,** Wadia Institute of Himalayan Geology, Dehra Dun, India; **YUDG-Mge,** University of Yangon, Department of Geology, Migyaungye (name of the Township, Magway Region, central Myanmar); **ZT,** Zhaotong collection, Yunnan Institute of Cultural Relics and Archaeology, Kunming, Yunnan Province, China.

Measurements Abbreviations

Measurements taken at first hand were made with digital calipers to the nearest 0.1 mm. Abbreviations are: c, lower canine; Hpara, paracone height; L, maximum mesiodistal length; Lbuc, buccal mesiodistal length; Lling, lingual mesiodistal length; Ltrigo, buccal maximum mesiodistal length of the m1 trigonid; m, lower molar; M, upper molar; MbucDling, maximum distance between mesiobuccal corner and distolingual corner of M1; MlingDbuc, maximum distance between mesiolingual corner and distobuccal corner of M1; p, lower premolar; P, upper premolar; W, maximum linguobuccal width; Wtalo, maximum linguobuccal width of the m1 talonid; Wtrigo, maximum linguobuccal width of the m1 trigonid.

Microcomputed Tomography and Postprocessing of 3-D Data

We used X-ray microcomputed tomography (μCT) at the University of Poitiers (France) (EasyTom XL Duo μCT, RX Solutions) to obtain digital data of the skulls of *Siamogale bounosa* (MM-54), and *Vishnuonyx maemohensis* (MM-78). The *Siamogale* skull was scanned at a voxel size of 41.0633 μm, voltage 90 kV and current 333 μA. The *Vishnuonyx* skull was scanned at a voxel size of 34.6071 μm, voltage 120 kV and current 250 μA. The 3D reconstruction was performed with Avizo Lite 9.5 (Visual Data Analysis, Zuse Institute Berlin and Thermo Fisher Scientific, United States) using a threshold value that permitted separating bones and teeth from coal matrix. After segmenting the upper teeth of MM-78 with Avizo, we stitched the broken teeth back together with Geomagic Studio (Geomagic Inc., Morrisville, NC) and positioned them to approximate the dental arch shape of an otter based on a skull of *Lutra lutra*. Three 3D models (one for the skull of *Siamogale*, one for the skull of *Vishnuonyx* and one for the stitched and repositioned upper teeth of *Vishnuonyx*) are available at MorphoMuseuM.com (Grohé et al., 2020).

Paleobiogeography

We performed faunal similarity analyses between Asian localities with terrestrial carnivorans during the middle and late Miocene. We first compiled faunal lists of localities from the literature, with geographic locations ranging longitudinally from Turkey to Japan, and latitudinally from Southeast Asia to southern Russia (see appendix S1 for complete faunal lists and appendix S2 for

list of references, in the supplementary data available online at doi.org/10.5531/sd.sp.40). We then removed doubtful taxonomic attributions (indet., aff., ?, sp.), singletons, and localities bearing only one taxon (see supplementary appendix S3, available online at doi.org/10.5531/sd.sp.40). We built a matrix of presence/absence of genera and species. We used both the Simpson and the Raup-Crick dissimilarity index to measure the difference in genus and species composition between localities. Those indices fulfil the richness independence criterion, in contrast to commonly used indices in ecology like Bray-Curtis, Sorensen, or Dice, which consider taxonomic richness as significant information on faunal structure (Kreft and Jetz, 2010). As the completeness of the fossil record is highly spatially and temporally heterogeneous, it is not appropriate to consider the richness of a locality as true information about the ecosystem. These differences in taxonomic composition between fossil localities coded within the dissimilarity matrices were represented in three ways. We used hierarchical clustering by UPGMA (Unweighted Pair-Group Method using Arithmetic average; *cluster* R package) and an ordination by NMDS (Non-Metric Multidimensional Scaling; *vegan* R package) directly on the matrix, as well as a hierarchical clustering on the NMDS coordinates; HCPC (Hierarchical Clustering on Principal Components; *FactorMineR* R package). Finally, computed clusters are analyzed with an analysis of similarity (ANOSIM) to test whether their respective faunas are significantly distinct (supplementary appendix S4, available online at doi.org/10.5531/sd.sp.40). This range of approaches allows us to avoid making overly strong assumptions about the structure of Miocene carnivoran faunas and the computed dissimilarity matrices (Brayard et al., 2007). We discussed these analyses taking into account the tectonic and climatic history of Asia. We excluded the early Miocene fossil record, too poor to be analyzed for Carnivora alone.

SYSTEMATIC PALAEONTOLOGY

Order Carnivora Bowdich, 1821

Suborder Caniformia Kretzoi, 1943

Superfamily Arctoidea Flower, 1869

Family Mustelidae Fischer, 1817

Subfamily Lutrinae Bonaparte, 1838

Siamogale Ginsburg et al., 1983

Type species: *Siamogale thailandica* Ginsburg et al., 1983.

Included species: *Siamogale thailandica* Ginsburg et al., 1983, *S. melilutra* Wang et al., 2018, *S. bounosa*, n. sp.

Diagnosis (from Wang et al., 2018: 41–42):

> *Siamogale* has typical lutrine cranial and dental morphologies: a large infraorbital canal, presence of antorbital fossa, uninflated bulla, robust and protruding mastoid process, mastoid process separated by a broad shelf from the paroccipital process, postglenoid foramen positioned

anteriorly to the auditory meatus, inion positioned anteriorly relative to the lambdoid crest, stylomastoid foramen separated by a bony ridge from the tympanohyal-bulla connection, masseter muscle attachment area ventrally expanded to beyond the ventral rim of the masseteric fossa, parallel zygomatic arches, shortened angular process, premolars with surrounding cingulum, shortening of P4 metastylar blade, presence of a notch between talonid and trigonid of m1, and widening of m1 talonid. *Siamogale* differs from *Paralutra jaegeri* by the presence of a distal ridge of m1 metaconid connected to the entoconid crest, M1 cuspule distal to metacone, and absence of P4 metastylar notch. *Siamogale* differs from *Paludolutra*, *Tyrrhenolutra* and *Enhydritherium* in having a crestiform protocone, lack of hypocone and presence of parastyle on P4, a distolingually expanded M1 talon, and metaconule placed distally to the metacone.

Geographical and stratigraphical distribution: Q–K and J lignite zones, late middle Miocene of Mae Moh Basin, Thailand (13.4–13.2 Ma and 12.8–12.2 Ma, respectively; Ginsburg et al., 1983; Grohé et al., 2010; this study); Shuitangba fossil site, latest Miocene of Zhaotong Basin, Yunnan Province, China (~6.2 Ma; Wang et al., 2018); Dapinggou, Pliocene Gaozhuang Formation of Yushe Basin, Shanxi Province, China (~4.9–5.4 Ma; Teilhard de Chardin and Leroy, 1945; Wang et al., 2018).

***Siamogale bounosa*,** new species

Figures 2–3, tables 1–2

Holotype: MM-54, nearly complete skull dorsoventrally compressed; on the left side, the zygomatic arch and the basicranial region are not preserved; on the right side, the region between the palatine and basioccipital is strongly damaged; right tympanic bulla partially preserved; left I1, C, P3–M1 and alveoli for I2, I3, P2; right I1, I3, C, P3, M1 and alveoli for I2, P2, P4; left i2 or i3; cervical vertebra; stored at PALEVOPRIM, Poitiers (France).

Etymology: From Greek *bounos* (masculine), "hill"; for the bunodont teeth morphology of this species.

Diagnosis: *Siamogale* with three upper incisors and three upper premolars on each side; P4 lingual shelf extended to the distal part of the metastyle; M1 with equally wide metacone and paracone buccal shelves. Differs from *S. thailandica* and *S. melilutra* in having equally developed buccal shelves of paracone and metacone on M1; from *S. thailandica* in having additionally a wider P3, a P4 with a slightly convex buccal wall, a nearly straight mesial wall, a more-extended lingual shelf, and an enlarged distolingual part of the M1 metacone; from *S. melilutra* in having additionally a narrower braincase where the mastoid processes do not extend to the level of the zygomatic arches, a more-cusped protocone and an hypoconal crest on P4, a P4 protocone more mesially located, a convex buccal border of P4, and an M1 paraconule running closer to the mesial border of the tooth.

Description: *Skull* (figs. 2–3; table 1): The skull has suffered from significant dorsoventral crushing leading to distortion of the premaxilla, maxilla, and nasal, and an overlapping of the right parietal and frontal on the left portions of these bones (fig. 2). On the left side, most of the region of the skull behind M1, including the zygomatic arch and the basicranial region, is missing. On the right side, the region between the palatine and basioccipital is partly lacking

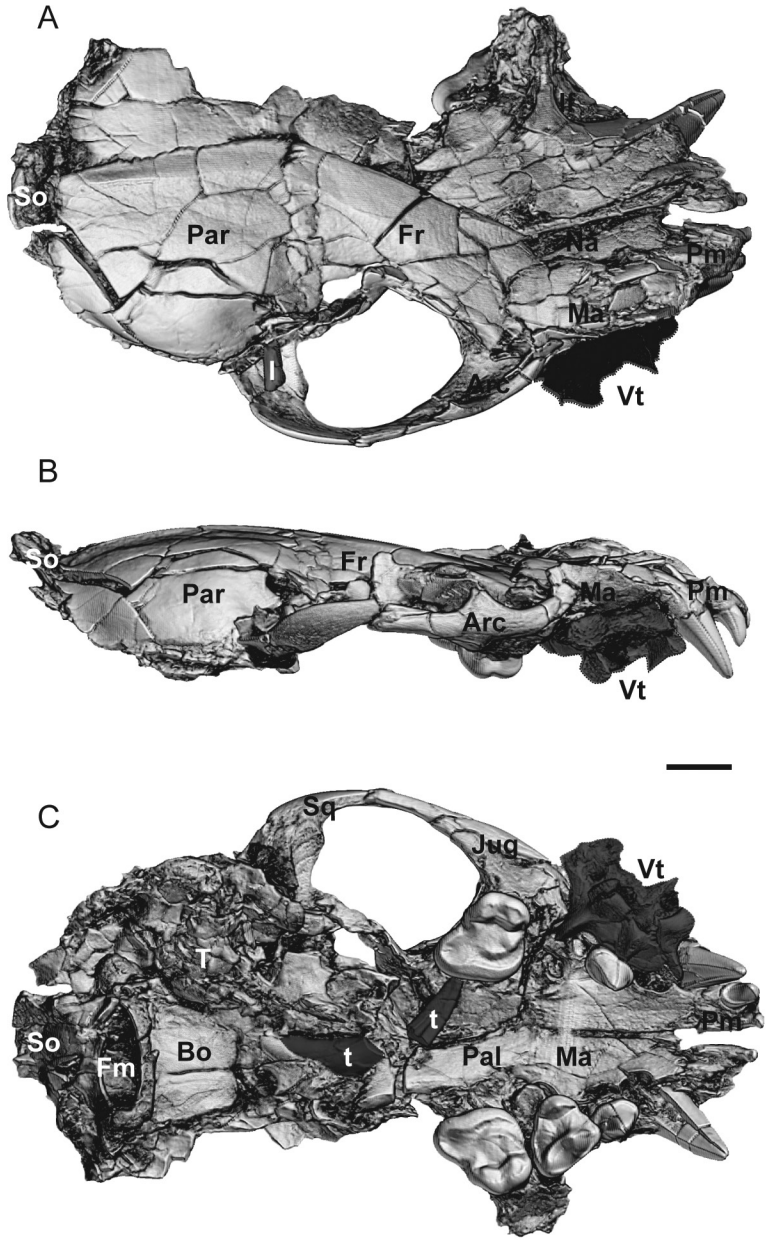

FIGURE 2. *Siamogale bounosa*, n. sp., MM-54, holotype skull. **A,** Virtual reconstruction in dorsal view; **B,** lateral view; **C,** ventral view. Abbreviations: **Arc,** zygomatic arch; **Bo,** basioccipital; **Fm,** foramen magnum; **Fr,** frontal; **I,** upper incisor 2 or 3; **If,** infraorbital foramen; **J,** jugal; **Ma,** maxilla; **Na,** nasal; **Pal,** palatine; **Par,** parietal; **Pm,** premaxilla; **So,** supraoccipital; **Sq,** squamosal; **T,** tympanic bulla; **t,** indeterminate tooth (probably belonging to a different species); **Vt,** cervical vertebra. Scale = 1 cm. Vt, I and t in darker grey.

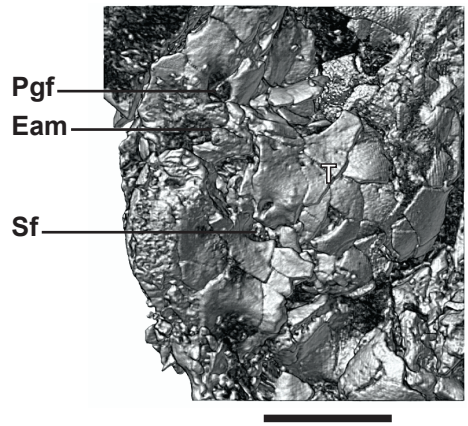

FIGURE 3. *Siamogale bounosa,* MM-54, skull holotype. Ventral view of the virtual reconstruction of the right basicranial region. Abbreviations: **Pgf,** postglenoid foramen; **Eam,** external auditory meatus; **Sf,** stylomastoid foramen; **T,** ectotympanic. Scale = 1 cm.

and otherwise broken into pieces. The auditory bulla is fragmented, but the lateral part of the ectotympanic and the external auditory meatus are still preserved (fig. 3). Due to the crushing, the foramina of the orbital region are not visible. In dorsal view, the nasal and premaxilla are collapsed with respect to the maxilla. Several displaced elements, probably from the same individual, are present on the skull: a cervical vertebra pressed against the buccal border of the right premolar row is visible in ventral view, and a left i2 or i3 is present in dorsal view, on the caudal part of the right zygomatic arch.

On the dorsal surface of the skull, the sutures between bones are not clearly visible. On its ventral surface, the suture between premaxilla and maxilla can be traced from the middle of the base of the canine lingual borders, the suture between maxilla and palatine can be seen especially on the left side of the skull close to the distolingual corner of M1, the suture between maxilla and jugal is observable buccal to the right M1 on the rostral portion of the zygomatic arch, and the suture between jugal and squamosal is distinct on the caudal half of the right zygomatic arch. *Siamogale bounosa* has a short and wide rostrum, as is typical in otters. Due to the deformation of the skull, neither the development of the postorbital process of the frontal nor the degree of the postorbital constriction can be evaluated. The infraorbital foramen is preserved only on the left side of the skull, but its shape and diameter cannot be evaluated accurately due to the crushing of the skull. In *Siamogale thailandica* and *S. melilutra*, the infraorbital foramen is oval, slightly wider dorsoventrally than laterally (TF 6296, Grohé et al., 2010: 1007, fig. 2g for *S. thailandica*; ZT-10-03-064b, Wang et al., 2018: fig. 4 for *S. melilutra*). The right zygomatic arch, rather thin and deep, is laterally curved, as opposed to its straighter condition in *S. melilutra* (ZT-10-03-064b, Wang et al., 2018: figs 2–4). It also bears a strong postorbital process of the zygomatic arch, as in *S. melilutra*. The dorsal surface of the skull exhibits no apparent sagittal crest, unlike in *S. melilutra*, but two weakly marked temporal crests. The right temporal crest is better preserved. It extends from the level of the rostral border of the orbit to the supraoccipital, by converging toward the break between the right and

TABLE 1. Cranial measurements of *Siamogale bounosa*, n. sp. (in mm).

Measurements	**MM-54**
Maximum skull length	115.9
Maximum skull width	70.4
Rostrum width	34.2
Length of the right dental row	51
Length of the left dental row	50
Length of the zygomatic arch	53.2

left parietal and frontal bones. The supraoccipital is elevated above the dorsal surface of the skull, which could be a result of the dorsoventral crushing. The nuchal crest is rather convex. The braincase is short, although longer than the rostrum, and is much narrower relative to the zygomatic arches. In ventral view, the right squamosal shows a short and wide glenoid fossa. A postglenoid foramen opens at the caudomedial base of the postglenoid process and at the rostrolateral corner of the external auditory meatus (fig. 3). The tympanic bulla is fragmented, but the ectotympanic is partially preserved and the external auditory meatus appears rather elongated. The bulla is inflated, and its surface is perforated by small pits on its rostral portion, as in specimen ZT-10-03-064b of *S. melilutra* (Wang et al., 2018: fig. 5A). The stylomastoid foramen is visible on the reconstructed digital skull on the caudolateral border of the bulla. Laterally and caudally to the bulla, the mastoid process is poorly developed ventrally and laterally, in contrast to the condition observed in *S. melilutra*, where the mastoid processes nearly extend to the level of the zygomatic arches and project much more ventrally.

Upper teeth (fig. 2; table 2): The left premaxilla bears I1 and the alveoli for I2–I3 whereas the right premaxilla bears I1 and I3 and the alveolus of I2. I1 shows a convex buccal border and a widened mesiolingual crown base. Its main cusp is relatively blunt. I3 has a convex buccal border, a main cusp displaced buccally relative to the long axis of the tooth and a lingual shelf. It is much larger than I1 and a cingulum is present mesially and lingually. The canines are sharp and weakly curved distally. They show longitudinal crests on their distal and mesiolingual faces. Behind the canines, the maxilla shows two alveoli for the P2, especially clearly visible on the right side. There is no P1. P3, preserved on both sides, is two-rooted, wide and short. It is slightly wider distally than mesially. It exhibits a sharp main cusp, slightly mesially placed with respect to the long axis of the tooth, and it bears two crests, mesial and distal, joining the crown base. A cingulum surrounds the tooth. It is thicker distally.

P4 is only preserved in the right maxilla. It is three-rooted (as seen by alveoli present on the left maxilla), triangular, and is slightly longer than wide. The tooth shows a convex buccal border, a nearly straight mesial border between the parastyle and protocone, and a lingual shelf extending until the distal end of the metastyle. The paracone mesial face is marked by two crests: one runs buccally to reach a weakly developed parastyle; the other runs lingually to join the base of the protocone. The paracone is much higher than the protocone and its tip is slightly distal relative to the protocone tip. Distal to the paracone, the carnassial notch is absent and the metastyle is short. On the lingual shelf, two crests separate the convex lingual face of

TABLE 2. Dental measurements (upper teeth) of *Siamogale* (in mm). Personal measurements and from [a]Grohé et al., 2010, [b]Wang et al., 2018.

	Siamogale bounosa		*S. thailandica*[a]		*S. melilutra*[b]				
	MM-54				ZT-10-03-064b		ZT-09-03-032		IVPP V 23272
Measurements	Left	Right	Range	Mean	Left	Right	Left	Right	Right
I1 L	2.4	2.5					5.09	5.22	
I1 W	2	2.1					4.13	3.98	
I2 L							5.82	6.02	
I2 W							4.68	4.5	
I3 L		5.6					8.19	8.31	
I3 W		4.2					5.79	6.12	
C L	5.9	5.7							
C W	6.9	5.6							
P2 L						10.7	10.02		
P2 W						6.6	5.4		
P3 L	8	7.2	7		12	11.8	11.57	11.94	
P3 W	5.4	5.3	4.1		8.1	7.6	7.51	8.07	
P4 L		11.7	11.1–13.5	12.08	16	15.7		14.81	
P4 W		10.7	8.5–11.1	9.68	15	15		14.43	
P4 Hpara		7.4	5.8–7.6	6.67					
P4 Hproto		3.3	3.2–4.8	3.82					
M1 Lbuc	9.9	9.9	8.5–12	9.73	14.6	14.2	13.19	13.18	13.65
M1 Lling	13	13.4	10.9–15.9	13.26	15.8	16	14.87	14.97	15.68
M1 W	14.1	14	12.3–17.8	14.53	17.4	17.6	17.37	17.47	17.2
M1 MlingDbuc	13.4	13.5	11.3–15.5	12.93					
M1 MbucDling	16.8	16.6	15.5–20.1	17.47					

the protocone from its flattened inner face. A weak crestiform hypocone lies just distal to the protocone. The enamel is wrinkled, particularly on the lingual shelf. A thin cingulum surrounds the tooth.

M1 bears low paracone and metacone. The widths of their buccal shelves are similar. The metacone is slightly shorter than the paracone. A metaconule is present on the distolingual border of the metacone. The paraconule and protocone are crestiform and separated by a distinct notch. Together they form a crescent-shaped blade extending distolingually from the mesial border of the M1 to the middle of the mesiodistal axis of the tooth. The distolingual border of M1 is enlarged. A cingulum surrounds the tooth, and the width of this cingulum is particularly important distolingual to the metacone and on the lingual border of the tooth, especially in its middle. As for P4, the enamel of M1 is wrinkled.

Additional elements appended to the skull (fig. 2): A left i2 or i3 is located on the dorsal side of the caudal part of the right zygomatic arch. At the base of the main cuspid a cingulid is present at the lateral and distal border of the tooth. A cervical vertebra caudal to the axis is tightly pressed against the right premolar region. An indeterminate fragmented tooth is partly embedded in the coal matrix on the ventral side of the skull. It is narrower than the upper canines and could correspond to a different individual or even to a different species.

Comparisons and discussion: MM-54 shows diagnostic morphological features of the genus *Siamogale*. Compared with the dental morphology of the type species *S. thailandica*, this new species exhibits a wider P3 relative to its length (table 2), a P4 with a slightly convex buccal border, a less-constricted area between the paracone and protocone, a more-extended lingual shelf, and an M1 with equally developed paracone and metacone buccal shelves and an enlarged distolingual part of the metacone. These morphological traits do not match the range of morphological variation observed among the numerous specimens attributed to *S. thailandica* from the same basin. Therefore, we attribute MM-54 to a new species. This taxonomic determination is consistent with the more recent age of MM-54 (J lignite zone, dated to 12.8–12.2 Ma) by comparison with the specimens of the type species *S. thailandica* (Q–K zones, dated to 13.4–13.2 Ma) discovered in the Mae Moh Basin. *S. bounosa* is a derived chronospecies of *S. thailandica*. In addition, *S. bounosa* differs from the more derived Chinese *S. melilutra* (Wang et al., 2018) in its smaller dimensions (tables 1–2), a narrower braincase where the mastoid processes do not extend to the level of the zygomatic arches, absence of a sagittal crest, a more-cusped protocone and the presence of an hypoconal crest on P4, a P4 protocone that is more mesially located, a buccal border of P4 that is convex rather than concave, equally developed buccal shelves of paracone and metacone on M1 rather than a more-developed paracone buccal shelf, and a paraconule running closer to the mesial border of M1.

The dental morphology of the type species *S. thailandica* recalls that of Galictinae, Lutrinae, and Melinae (Grohé et al., 2010). However, *Siamogale bounosa* shows a more-derived dentition compared with the type species, with a lingual shelf of P4 reaching the end of the metastyle associated with equally developed buccal shelves of the paracone and metacone of M1, which are clearly different from the dental features observed in extant and fossil galictines (e.g., *Lutravus*, *Trigonictis*, *Sminthosinis*, *Enhydrictis*, *Pannonictis*). Moreover, the reduction in P4 length with an extension of the lingual shelf beyond the metastyle blade is different from the condition observed in the extant badgers *Meles* and *Arctonyx*. The shape of the P4 protocone of *S. bounosa* is also crestiform, as opposed to cusped in *Meles* and reduced to a bulge in *Arctonyx*. Finally, increasing morphological evidence of a relationship between *Siamogale* and other fossil lutrines support its belonging to this subfamily (Wang et al., 2018).

Vishnuonyx Pilgrim, 1932

Type species: *Vishnuonyx chinjiensis* Pilgrim, 1932.

Included species: *Vishnuonyx chinjiensis* Pilgrim, 1932, *V. angololensis* Werdelin, 2003, *V. maemohensis*, n. sp.

Diagnosis (from Pilgrim, 1932: 93–94):

> Lutrinae of rather small size; having a P4 of triangular shape; antero-posterior diameter on the outer side much exceeding that on the inner side, and also much exceeding the transverse diameter; with a high, pointed paracone; metacone lower but elongated; parastyle weak; with two internal cusps, protocone and hypocone, both much lower than the paracone; protocone situated rather far forward; with a slight internal cingulum; M1 rather small; mandible with a deep ramus; p4 elongate, only slightly broader posteriorly; with a strong posterior accessory cusp, not situated so much to the outside of the main cusp as in *Sivaonyx*, without an anterior accessory cusp; with a broad cingulum; m1 with talonid broader and shorter than trigonid, surrounded by a crenulated rim, of which the entoconid is as strong as the hypoconid; m2 elongate oval, rather longer than in *Sivaonyx*.

Remarks: Because of the inclusion of a new species of *Vishnuonyx* from Thailand and of the description of some material of *V. chinjiensis* (type species) from Pakistan further below, we add some remarks to the diagnosis of Pilgrim: a small mesial accessory cuspid is present on the p4 of *Vishnuonyx*, the m1 talonid is slightly narrower than the trigonid, the entoconid is lower than the hypoconid, and the presence of a crenulated rim surrounding the talonid as well as the depth of the mandibular ramus (i.e., as deep as or deeper than the m1 length) are variable within specimens of the genus.

Geographical and stratigraphical distribution: R and Q–K lignite zones, late middle Miocene of Mae Moh Basin, Thailand (14.2–14.1 and 13.4–13.2 Ma, respectively; this study); Middle Miocene of Chinji Formation, Potwar Plateau, Pakistan (~14–11.4 Ma; Pilgrim, 1932); Middle Miocene of Ramnagar, India (~13.8–13.2 Ma; Nanda and Seghal, 1993); Middle Miocene Locality 2/11, Kabarsero, Member D, Bed 3, Ngorora Formation, Kenya (~12 Ma; Morales and Pickford, 2005); Late Miocene of the lower member of the Nawata Formation, Lothagam, Kenya (7.1±0.1–6.5±0.1 Ma; Werdelin, 2003); Late Miocene of Haradaso Member, Sagantole Formation, Middle Awash, Ethiopia (4.85–5.2 Ma; Haile-Selassie, 2008).

***Vishnuonyx maemohensis*,** new species

Figures 4–5, tables 3–5

Holotype: MM-30, right mandible with c, p3–m2 and alveoli for p1–p2, and left mandible with c–m2 from the same individual; stored at the DMR, Bangkok.

Referred material: MM-32, left mandible (m1); MM-33, left mandible (p4–m1, alveolus for m2); MM-34, left mandible (p2–m1, alveolus for m2); MM-35, right mandible (p3–m1, alveoli for p2 and m2); MM-36, right P4; MM-37, left M1 (all stored at the DMR, Bangkok); MM-78, rostral part of a skull broken at the level of the glenoid fossae and right zygomatic arch missing; on the right side: I1–I2, alveoli for I3–C poorly visible, P1–M1, on the left side: alveoli for I1–I2 poorly visible, I3, alveolus for C, P1–M1; MM-79, right mandible (partial distal root for p3, broken roots for p4 and m1, and alveolus for m2) (both stored at PALEVOPRIM, Poitiers, France).

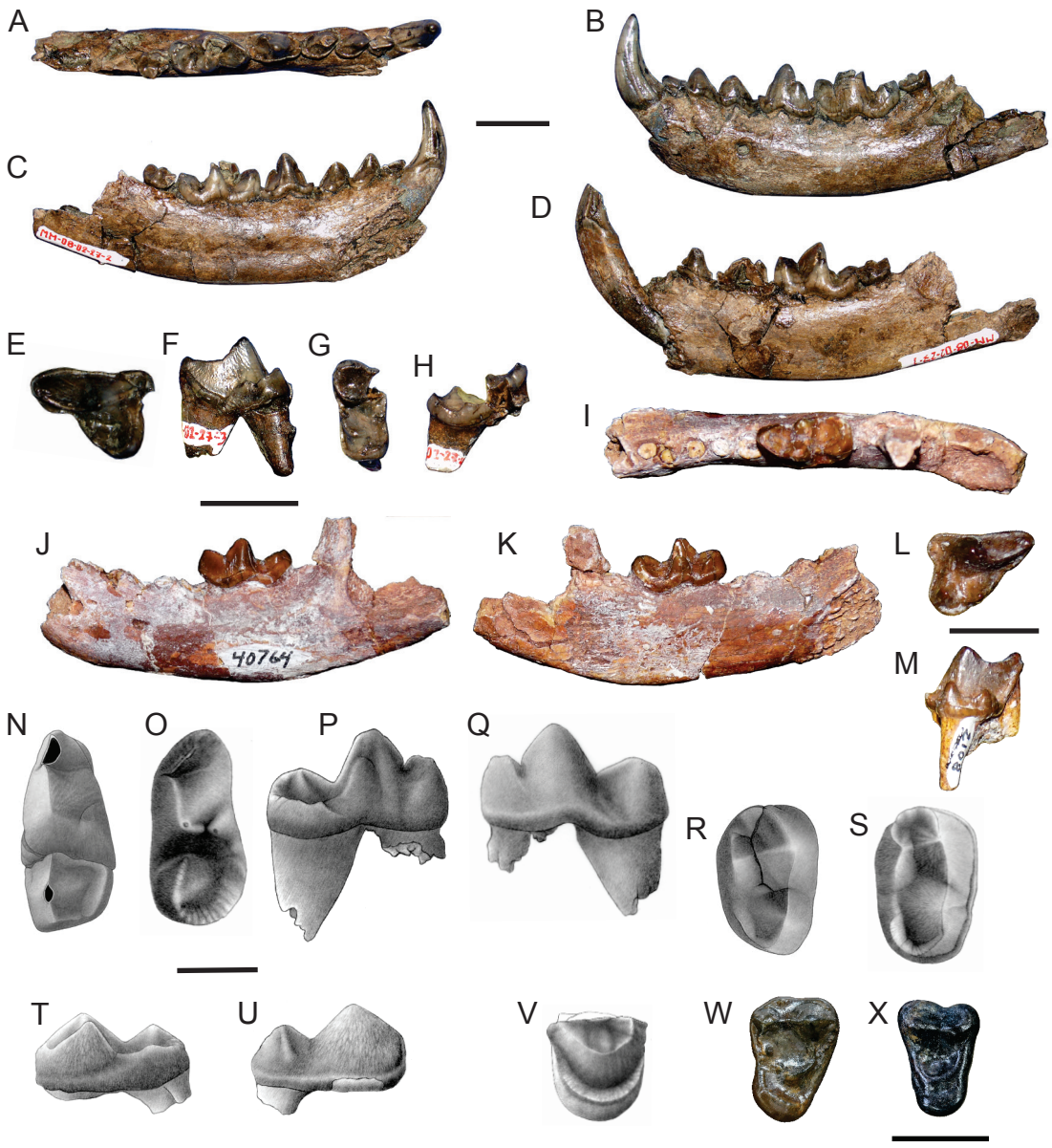

FIGURE 4. *Vishnuonyx maemohensis,* n. sp., from Mae Moh Basin: **A,** occlusal, **B,** buccal, and **C,** lingual views of the left mandible, MM-30, holotype; **D,** lingual view of the right hemimandible, MM-30, holotype; **E,** occlusal, **F,** lingual views of right P4, MM-36; **G,** occlusal, **H,** distal views of left M1, MM-37. *Vishnuonyx chinjiensis* from northern Pakistan: **I,** occlusal, **J,** buccal, **K,** lingual views of left mandible GSP-Y 40764, loc. Y828, Chinji Formation; **L,** occlusal, **M,** lingual views of left P4 GSP-Y 2108, loc. Y53, Chinji Formation. *Maemohcyon potisati* from Mae Moh Basin: **N,** occlusal view of left m1, TF 6210, holotype; **O,** occlusal, **P,** lingual, **Q,** buccal views of left m1, MM-38; **R,** occlusal view of left m2 (reversed here), TF 6210, holotype; **S,** occlusal, **T,** lingual, **U,** buccal views of right m2, MM-39. ?*Maemohcyon potisati* from Mae Moh Basin: **V,** occlusal view of right M1, MM-40; **W,** occlusal view of right M2, MM-77. cf. *Pseudarctos* sp. from Mae Moh Basin: **X,** occlusal view of left M1, MM-41. N and R from Peigné et al. (2006). Drawings by Sabine Riffaut. Scale = 1 cm for A–D and E–H, I–M, N–W, X.

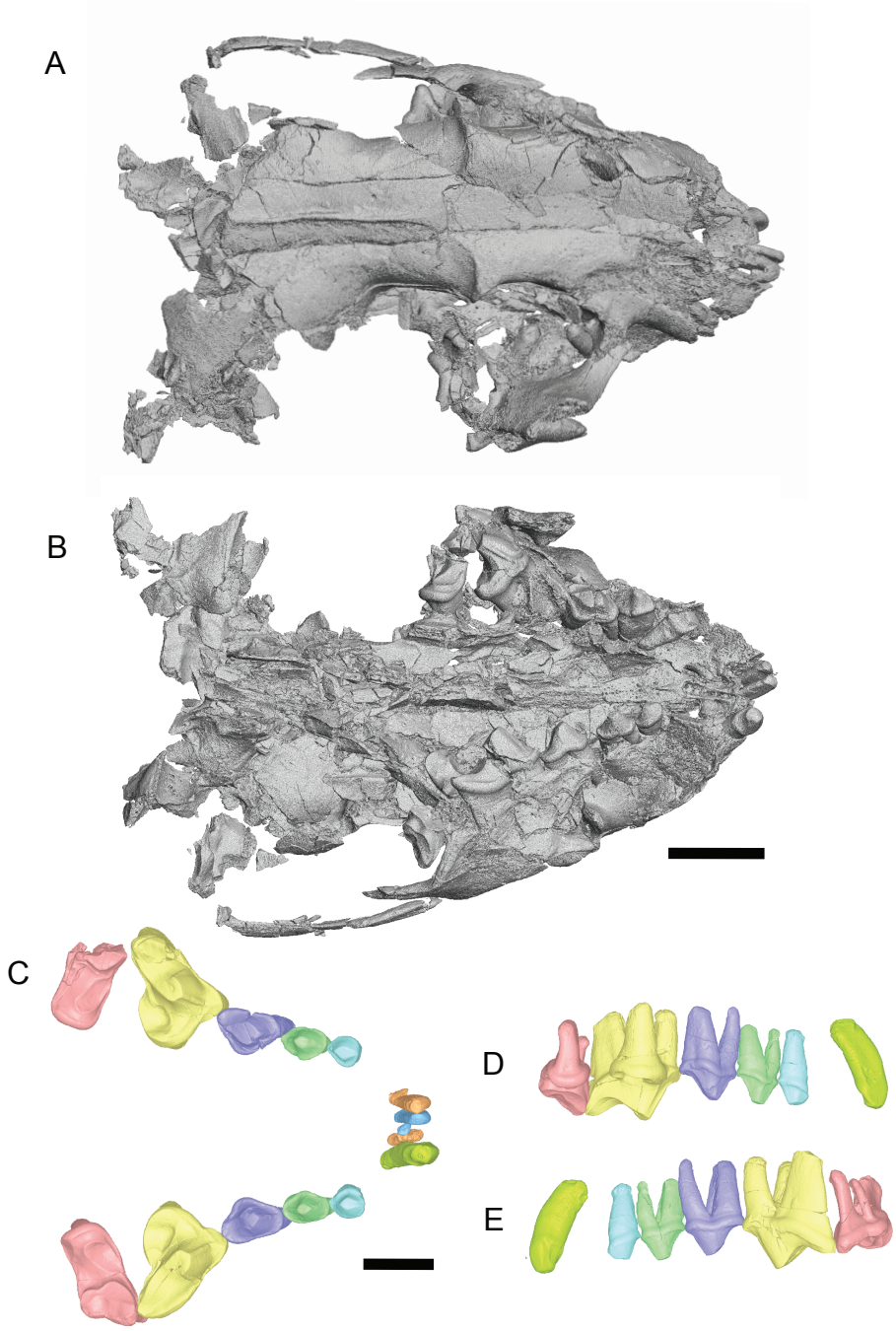

FIGURE 5. *Vishnuonyx maemohensis*, virtual reconstruction of the skull and upper teeth MM-78. **A,** dorsal, **B,** ventral views of the skull; **C–E,** upper teeth extracted virtually (including roots of left I1–I2), broken pieces stitched back together. **C,** occlusal view (for an easier visual representation, the shape of the dental arch approximates that of a modern river otter); **D,** lingual and **E,** buccal views of the left upper teeth, from I3 to M1. Scale = 1 cm for A–B and C–E.

TABLE 3. Dental measurements (lower teeth) of Asian and African *Vishnuonyx* and *Torolutra* species (in mm). Personal measurements and from [a]Pilgrim, 1932, [b]Petter et al., 1991, [c]Morales et al., 2005, [d]Pickford, 2007, [e]Haile–Selassie, 2008, [f]Peigné et al., 2008. * Measurements from alveoli or crown base and estimations from broken teeth.

	c	p1	p2	p3	p4	m1	Ltrigo	Wtrigo	Wtalo	m2
Vishnuonyx maemohensis										
MM-30 (holotype) left	6.2×4.5			6.2×3.7	8.3×?	11.8×6.2	7.8	6.2	5.8	4.5×4.2
MM-30 (holotype) right	6×4.5	3.5×2.6	5.3×3.1	6.1×3.7	8.2×4.6	11.9×6	7.8	5.8	5.6	4.5×4.2
MM-32						12.1×6.4	7.8	6.1	5.8	
MM-33					7.6×4.1	10.6×5.8	6.7	5.3	4.7	
MM-34			5.1×2.9	5.3×3.1	6.7×3.5	10.5×5.2	7.1	5.2	4.2*	
MM-35				5.2×3.4	7.7*×?*	11.1×5.8	7.3	5.8	5.2	
MM-79					7.1*×3.5*	10.7*×4.8*				3.4*×2.3*
V. chinjiensis										
GSI D 245[a]					7.3×4.2	11.7×?				5.0×3.3
WIHG FR 24/18[d]					7.2×4.3					
GSP-Y 40764						12.2×5.9	7.5	5.8	5.7	
Vishnuonyx sp.										
GAW-VP-1/1[e]						13.5×7.2	8.2			
Torolutra ougandensis										
NK 415′87 (holotype)[b]					9.8×6.3	16.4×8.4	11		8.4	
NK 635′86[b]					10×6.4					
BAR 348′00[c]						15.8×7				
BAR 534′99[c]					9.6×6.5					
GAW-VP-1/5[e]					8.7×5.1	13.4×6.9	8,2			
GAW-VP-1/146[e]						13×6.7	7,9			
GAW-VP-1/173[e]	7.3×6.5									
GAW-VP-3/25 (right)[e]	8.8×6.5					15.3*×7.5*				
GAW-VP-3/25 (left)[e]	8.7×6.6									
aff. *Torolutra* sp.										
TM 266-01-194[f]				6.8×3.8	9.5*×?	16×?	10.5		7.5	

TABLE 4. Cranial measurements of *Vishnuonyx maemohensis*, n. sp. (in mm). * Maximum length for the remaining broken parts.

Measurements	**MM-78**
Maximum skull length	85.7*
Maximum skull width	56.1*
Rostrum width	33.9*
Length of the zygomatic arch	47.1*

TABLE 5. Dental measurements (upper teeth) of Asian and African *Vishnuonyx* species (in mm). Personal measurements and from [a]Werdelin 2003, [b]Morales and Pickford 2005, [c]Pickford 2007. The upper teeth of MM-78 have been measured on the 3D reconstructions with Geomagic Studio. * Estimated.

	Vishnuonyx maemohensis				*V. chinjiensis*			*V. angololensis*
	MM-36	MM-37	MM-78		GSI D 223[c]	GSP-Y 2108	KNM-BN 1730[b]	KNM-LT 23948[a]
Measurements			Left	Right	(holotype)			
I1 L				2.7				
I1 W				1.3				
I2 L				2.5				
I2 W				1.5				
I3 L			3.7					
I3 W			2.3					
P1 L			4	3.8				
P1 W			3.2	3.2				
P2 L			5	5.1				
P2 W			3.3	3.4				
P3 L			6.5	6.7				
P3 W			4.5	4.6				
P4 L	12.2		11.9	11.7	11.5	10.2	11.6	15.3
P4 W	8.6		8.3	8.4	9.1	7.8	9.4	12.9
P4 Hpara	7.8		5.7*	5.8*	7.4	5.9	7.4	
M1 L		5.3*	5.9	5*				
M1 W		11.1	11.5					
M1 MlingDbuc			9.7					
M1 MbucDling		11	11.7					

Etymology: The species name derives from the locality where it was originally found, Mae Moh.

Diagnosis: *Vishnuonyx* with p1 present; protoconid of m1 much higher than metaconid, metaconid displaced distally relative to protoconid, talonid narrower than trigonid, high hypoconid, talonid basin poorly developed, talonid distal border oriented distobuccally; m2 with high metaconid, aligned and oblique paraconid-protoconid-hypoconid, talonid distal border oriented distolingually; P4 with protocone distal crest bearing a tiny cusp, thick lingual cingulum at the metastyle base; M1 transversely widened, small metaconule, paraconule-protocone blade, poorly developed distolingual cingulum.

Differential Diagnosis: Differs from *V. chinjiensis* and *V. angololensis* in having a P4 with a thinner cingulum at the base of the lingual cusps and a thicker one lingual to the metastyle end; from *V. chinjiensis* additionally by a shallower mandibular ramus, a larger P4 bearing a notch rather than a U-shaped valley between the protocone and hypocone; from *V. angololensis* additionally by a smaller P4 having a more distinct parastyle.

Description: *Mandible and lower dentition* (fig. 4; table 3): The left mandible of the holotype MM-30 bears c–m2. Only the horizontal ramus is preserved. The masseteric fossa is moderately deep and extends below the distal part of m2. In buccal view, two mental foramina open beneath the p1–p2 contact and the distal part of p3. In lingual view, the mandibular symphysis extends caudoventrally until the distal part of p3. The teeth are set close together and are oriented mesiobuccally from the canine to the p3. The p1 and m2 are single-rooted. Two thick longitudinal crests extend from the canine tip and run on the middle of its lingual and distal faces to join the basal cingulid. Another, thinner one, runs on the canine buccal face. There is a lingual and distal cingulid. The p1 is much lower than p2 and p3, which have approximately the same height. The p4 is twice as high as p2 and p3. The p1–p3 are built on the same pattern: the main cuspid is mesial relative to the crown length and two crests extend mesially and distally until reaching the base of the crown. The p4 bears a tiny mesial accessory cuspid and a high and distinct distal accessory cuspid that reaches the mid-height of the main cuspid. The p4 distal accessory cuspid is displaced buccally relative to the main cuspid and is slightly lower than the m1 paraconid in buccal view. From p1 to p4, the main cuspid tends to be more distal and the cingulid surrounding the premolars thickens to form a distal cingular shelf in p4. The m1 trigonid is longer than the talonid. The m1 paraconid, which bends lingually, is lower than the main cuspid of p4. The right mandible of the holotype shows an unbroken m1 protoconid, which allows a more-detailed description of the trigonid morphology. The paraconid has approximately the same length as the protoconid, the latter being the highest cuspid of m1. The metaconid reaches approximately the same height as the paraconid. The paraconid has a distolingual crest that is half as long as the distobuccal crest. This short distolingual crest of the paraconid and the rather distal position of the metaconid relative to the protoconid create a wide trigonid lingual valley. The metaconid has a straight distal face that abruptly meets the lingual talonid, as commonly observed in otters. The protocristid is shorter than the paracristid. The talonid is much lower and slightly narrower than the trigonid. The cristid obliqua extends distolingually from the base of the protoconid to join a sharp and

high hypoconid. The distal border of the tooth is straight and distobuccally oriented. The entoconid crest is lower than the hypoconid. The talonid is poorly basined. A cingulid is present on the buccal and mesial side of the tooth. It is thinner on the lingual side where it ends behind the paraconid. The m2 is very small and slightly longer than wide. The paraconid, protoconid, and hypoconid are obliquely aligned. The metaconid is high, located at the mediolingual side of the molar, and is displaced distally relative to the protoconid. The partially broken paraconid is close to the protoconid. The cristid obliqua extends distobuccally from the distal base of the protoconid to the hypoconid. The distal border of the tooth has a distolingual orientation, opposite to that of m1. The cingulid is visible on both the buccal and lingual sides of m2.

Skull (fig. 5; table 4): The skull is heavily compressed and teeth point toward the right side: the left side of the jaws folds medially, so that the upper premolars and molars sit against the maxilla while the right side is displaced laterally. The ventral floor of the skull, from the premaxilla to the pterygoid, is broken into many pieces. On the premaxilla, the incisive foramina are elongated. The maxilla and palatine regions are collapsed inside the skull. The rostroventral and rostrodorsal branches of the zygomatic arches are broken off and sit tightly against each other such that the outline of the infraorbital foramen is not fully visible. On the left side, only the caudal part of the zygomatic arch attached to the glenoid fossa is missing. The zygomatic arch appears thin behind the postorbital process. On the right side, the zygomatic arch is missing behind the infraorbital foramen. The basicranial region is not preserved, but part of the left tympanic bulla has been displaced rostrally to the glenoid fossa. In dorsal view, the rostrum is short, the postorbital processes of the frontal are marked, and a low but distinct sagittal crest is present. From the size and general proportions of the skull, *V. maemohensis* appears as large as a modern river otter.

Upper dentition (fig. 5; table 5): Most of the upper teeth are preserved on the skull. *V. maemohensis* has three upper incisors, as indicated by the right I1 and I2 and left I3. I1 and I2 are very similar in size, with I2 slightly larger, and both show a single spatulate main cusp. I3 is larger than I1 and I2. The I3 crown is higher; the tip of the main cusp is located buccally and the crown widens at the distolingual base of the tooth. I3 is surrounded by a cingulum that becomes thinner buccally. No canines are preserved. The alveolus for the left canine is less deformed than the one for the right canine and is oval. P1–P3 show the same general morphology: a main cusp from which two crests extend mesially and distally, a lingual bulge and a basal cingulum surrounding the tooth. The tip of the P1 main cusp is mesially displaced relative to the tooth length; this cusp is less mesially displaced in P2 and lies in the middle of the tooth in P3. The lingual bulge, small in P1, gets wider in P2 and almost creates an extra root mesiolingually to the distal root in P3. The skull teeth showing strong wear, the morphology of P4 and M1 is better preserved on the isolated specimens MM-36 and MM-37. P4 has a long metastyle and a high paracone from which two crests extend mesially. The mesiobuccal one joins a low and sharp parastyle and the mesiolingual one joins the base of a high protocone, forming a wide U-shaped valley in mesial view. The protocone is displaced mesially with respect to the paracone and distally relative to the parastyle. The hypocone lies distolingually to the paracone and distobuccally to the protocone. It is half the height of the protocone and

closer to the lingual border of the carnassial. The distal crest going down from the protocone bears a very low cusp near the notch separating the two lingual cusps. These cusps delineate a relatively broad lingual shelf, which does not extend to the distal end of the metastyle, contributing to a triangular P4. The distal crest going down from the hypocone meets the lingual cingulum at the middle of the metastyle lingual face. The lingual cingulum, well marked at this level, is thicker than the buccal one. M1 specimen MM-37 is broken at its distobuccal corner such that the metacone is not preserved. The tooth is wide transversely and the mesial and distal borders are roughly parallel. The cusps are high and sharp. The parastyle and the paracone buccal shelf are moderately developed. Directly lingual to the paracone, a paraconule-protocone blade arises from the mesial border of the tooth to run lingually and gently distally. The paraconule is lower than the protocone. A very shallow notch separates these two cusps. A small and very distal metaconule is present lingual to the metacone region. It is lower than the paraconule. The distolingual cingulum is poorly developed, but thicker than the buccal and mesial ones. On the skull specimen MM-78, the left M1 still preserves the buccal region. The metacone is shorter than the paracone and its buccal shelf is less developed than the buccal shelf of the paracone.

Comparisons and discussion (tables 3–5): *Vishnuonyx* was represented by two species so far: *V. chinjiensis* Pilgrim, 1932, and *V. angololensis* Werdelin, 2003. The type species *Vishnuonyx chinjiensis* was originally described from a left maxilla with P4 and a fragment of the root of M1 from the middle Miocene of the Chinji Formation, in the Potwar Plateau of northern Pakistan (Pilgrim, 1932). Another P4 attributed to this species is reported from the middle Miocene of the Ngorora Formation, Kenya (Morales and Pickford, 2005). We compared MM-36 with the holotype of *V. chinjiensis* (GSI D 223, Pilgrim 1932: pl. II, figs. 17–17A; Pickford, 2007: fig. 3A; only the P4 figured) and to a better preserved and yet undescribed P4 from the Potwar Plateau of northern Pakistan displaying similar proportions, morphology, and age as the holotype (GSP-Y2108 from loc.Y53 dated to 12.756 Ma based on the timescale of Gradstein et al., 2012; here attributed to *V. chinjiensis*, fig. 4L–M). The P4 of *V. maemohensis* is different from that of *V. chinjiensis* in being longer relative to its breadth (table 5), in displaying a notch between the protocone and hypocone rather than a U-shaped valley, and in having a lingual cingulum thicker at the level of the metastyle than at the level of the protocone-hypocone compared with a similarly developed cingulum on those regions for *V. chinjiensis*. The Mae Moh upper carnassial also differs from the Kenyan P4 of *V. chinjiensis* (Morales and Pickford, 2005: 278, fig. 4A) in being longer and narrower and in exhibiting a deeper separation between the protocone and hypocone. In addition to the holotype, Pilgrim (1932) describes and figures a mandible fragment of *V. chinjiensis* found in the same beds near Chinji (GSI D 245, Pilgrim, 1932: pl. IV, figs. 6–6a). This mandible preserves only p4, a part of m1 talonid, and a fragment of m2 (ramus with p4 refigured by Pickford, 2007: 88, fig. 3). The p4 bears a strong distal accessory cuspid and the m1 talonid has a narrow basin with a distinct hypoconid, as in the Thai specimens. Although described as absent by Pilgrim (1932), a tiny mesial accessory cuspid merging with the cingulid of p4 is visible on GSI D 245, as in the Thai material. Moreover, Pilgrim (1932) described the m1 talonid of *V. chinjiensis* as wider than the trigonid based on

this specimen. However, the m1 trigonid is lacking and only the mesial alveolus for the trigonid is visible, so that the relative proportions of m1 talonid and trigonid cannot be inferred. In *V. maemohensis* the m2 is shorter and wider than in GSI D 245, while the m1 and p4 have the same range of dimensions, although the p4 might have been slightly longer than in *V. chinjiensis* relative to its width (table 3). We also compare *V. maemohensis* specimens to another yet undescribed specimen from the Chinji Formation of the Potwar Plateau displaying similar proportions, morphology and age as GSI D 245 but with a completely preserved m1 (GSP-Y 40764 from loc. Y828 dated to 13.357 Ma based on the timescale of Gradstein et al., 2012; here attributed to *V. chinjiensis*, fig. 4I–K). It is very similar to *V. maemohensis* in morphology, but the m1 is narrower relative to its length and the depth of the mandible below m1 is greater relative to m1 length than in *V. maemohensis*. The type species of *Vishnuonyx* is also recorded in the middle Miocene of Ramnagar, India, by a mandibular fragment with p4 (Nanda and Sehgal, 1993). For the same width, the p4 of *V. maemohensis* is longer than in the Indian specimen (table 3).

Vishnuonyx angololensis is reported by a P4 from the late Miocene of the lower member of the Nawata Formation of Lothagam, in Kenya (Werdelin, 2003). MM-36 is closer to that specimen than to the material of *V. chinjiensis* by the presence of a notch between the protocone and hypocone. It has, however, smaller dimensions and is narrower relative to its length, and it bears a more distinct parastyle and a thinner lingual cingulum at the base of the lingual cusps compared with the P4 of *V. angololensis*.

Haile-Selassie (2008) attributed a mandible from the earliest Pliocene of the Haradaso Member, Sagantole Formation, Middle Awash (Ethiopia) to *Vishnuonyx* sp. He stated that this specimen could belong to *V. angololensis* based on the temporal and spatial proximity between Lothagam and Middle Awash. *V. maemohensis* differs from this material in displaying smaller proportions, a higher protoconid, a longer trigonid relative to m1 length, a wider lingual trigonid valley, and in having a shallower mandibular ramus.

We also compare *V. maemohensis* to some *Torolutra* specimens, as it has been suggested that *V. angololensis* might belong to this genus (Haile-Selassie, 2008). *Torolutra ougandensis* was first reported from mandibular fragments and a lower canine from the lower Pliocene of Nyaburogo, Nkondo and Warwire Formations, Uganda (Petter et al., 1991). Compared with this material, the lower teeth of *V. maemohensis* are shorter and narrower, the cingulid is thinner, especially on the buccal side of p4, and the m1 has a narrower paraconid, a wider lingual valley of the trigonid, and a narrower and deeper talonid basin. Additional material of *Torolutra ougandensis*, including a P4, is described from the late Miocene Kapcheberek locality, Lukeino Formation of the Tugen Hills, Kenya (Morales et al., 2005). MM-36 differs from it in being shorter and narrower relative to its length, and in having a notch rather than a valley separating the protocone and hypocone, a thicker lingual cingulum at the region of the metastyle and thinner cingulum surrounding the lingual cusps. Specimens referred to *T. ougandensis* by Haile-Selassie (2008) from the latest Miocene of Adu-Asa Formation and earliest Pliocene of Sagantole Formation (Asa Koma and Haradaso members, respectively) of the Middle Awash, Ethiopia, bring additional morphological information. The lower canine of *V. maemohensis* is less robust at its base, and its crown is less

convex in its proximal half compared with GAW-VP-3/25 (Haile-Selassie 2008: 560, fig. 3G). The maxillary fragment GAW-VP-1/3 bears an M1, which is described but not figured by the authors: "A strong shelf-like cingulum is present on the buccal side of the paracone and metacone, larger at the former. The crown also has a deep, centrally positioned median valley. The paracone and metacone are of equal height and separated by a V-shaped valley" (Haile-Selassie, 2008: 562). This description, relatively common for otter species, does not allow comparisons with the material of Mae Moh. However, the M1 of *V. maemohensis* is shorter and wider than this specimen. Moreover, the authors also figured and described an M1 from the Asa Koma Member of the Adu-Asa Formation of the Middle Awash assigned to Lutrinae indet. aff. *Torolutra* sp. (ASK-VP-3/411). MM-37 differs from it in being wider relative to its length, in having a paraconule (absent in ASK-VP-3/411, according to Haile-Selassie, 2008, maybe because of wear), in having higher and sharper cusps, a protocone more distant to the lingual border of the tooth, a thinner cingulum at the mesiobuccal and distolingual borders of the tooth, and a narrower lingual root.

The difference in morphology and measurements between the upper carnassial from Mae Moh and those of *V. chinjiensis* and *V. angololensis* are important enough to erect a new species. *Vishnuonyx maemohensis* is the oldest and could be the most primitive species of the genus (e.g., high protoconid, narrow talonid basin on m1, narrower P4 with distinct parastyle). The Thai specimens described here highlight the closer morphological resemblance between *Vishnuonyx* and the African Mio-Pliocene and early Pleistocene *Torolutra* (see Werdelin and Peigné, 2010, for a list of localities; Werdelin and Lewis, 2013) than to the African and Eurasian Mio-Pleistocene *Sivaonyx-Enhydriodon*. The primitive morphology of *V. maemohensis* and the oldest presence of *Vishnuonyx* in the African continent at ca. 12 Ma (Morales and Pickford, 2005) could confirm a dispersal event of the genus from Asia to Africa during the middle Miocene, probably between ca. 12 and 14 Ma (Grohé et al., 2012).

Family Amphicyonidae Haeckel, 1866

Subfamily Amphicyoninae Haeckel, 1866

Maemohcyon Peigné et al., 2006

Maemohcyon potisati Peigné et al., 2006

Figure 4, table 6

Holotype: TF 6210, fragment of left hemimandible with m1, and isolated left fragmentary canine, p4, m2 lacking its distalmost part, and right m2. This material belongs to a single, young adult individual and is stored at the DMR, Bangkok.

Referred material: MM-38, left m1 and MM-39, right m2; both stored at the DMR, Bangkok.

Diagnosis (from Peigné et al., 2006: 529):

> Mid-sized amphicyonine differing from the typical species of *Amphicyon* (mainly European and North American species) by teeth that do not display the diagnostic 'swollen inflated appear-

ance' (Hunt, 2003, p.82) and by a less reduced p4 relatively to m1 (compared with middle Miocene *Amphicyon*) and an enlarged m2 relatively to m1 (compared to early Miocene *Amphicyon*). Compared to *Cynelos*: m1 talonid with a less developed entoconid and a less pronounced basin; much enlarged (relatively to m1), less rectangular m2 with a narrower talonid that tapers distally and a more prominent hypoconid. Compared to *Ysengrinia*: much enlarged m2 relatively to m1, m2 broader than m1 (except in *Y. depereti*). Compared to *Pseudocyon*: less reduced p4 and enlarged m2 (both relatively to m1), m2 with trigonid cusps not mesially shifted (trigonid longer than talonid) and with a prominent hypoconid crest. Compared to *Pliocyon*: enlarged m2 relatively to m1. Compared to *Ischyrocyon* (especially late Miocene specimens): narrower and less reduced (relatively to m1) p4; distal accessory cusp present on p4, m1 retaining a metaconid and having a buccally placed hypoconid.

Description (fig. 4O–Q, S–U): The trigonid of m1 is longer and slightly narrower than the talonid. The paraconid is very mesial, short and narrow. Its tip is nearly aligned with that of the protoconid. The metaconid is approximately as high as the paraconid and lower than the protoconid. It is partly fused to the lingual face of the protoconid and displaced distally relative to the tip of the protoconid. The mesial crest of the metaconid is very short. The distal face of the protoconid and metaconid is oblique. The talonid bears a high and slightly distobuccally oriented cristid obliqua. This crest starts from the protoconid base to join a strong hypoconid at two-thirds of the talonid length. The hypoconid is slightly lower than the metaconid and paraconid. The distal crest of the hypoconid is reduced in height abruptly distolingually to reach half the hypoconid height. It continues into an entoconid crest that gently curves along the distal and lingual borders of the talonid to reach the base of the metaconid distal face. The entoconid crest is crenulated distally. The talonid is unbasined. The lingual face of the hypoconid and cristid obliqua is oblique and weakly concave whereas the lingualmost part of the talonid is roughly horizontal. The cingulid is poorly visible. It is more developed on the buccal side of the talonid. The dorsalmost part of the buccal face of the paraconid, the mesialmost part of that of the protoconid, and the dorsodistal corner of the buccal face of the hypoconid show shearing facets.

The m2 is wider and shorter than m1. The m2 trigonid is wider than the talonid. It shows a very low vestigial paraconid from which two curved crests extend distally. Whereas the distobuccal crest joins the protoconid tip, the distolingual one interrupts its course on the metaconid mesial face, just below its tip. The protoconid is the highest trigonid cuspid. Compared with the m1 metaconid, the m2 metaconid is larger (clearly separated from the protoconid), higher (but still lower than the protoconid) and less distal relative to the protoconid. Protoconid and metaconid are linked by a short V-shaped crest. A distal crest extends from the metaconid tip to below the middle of its distal face. The talonid is lower than the trigonid. The cristid obliqua is oriented slightly distolingually and joins a distal crest going down from the protoconid tip at an approximately right angle. The hypoconid is strong, approximately as high as in m1. Compared with m1, the distal crest of the hypoconid becomes lower less abruptly and the entoconid crest extends only until it reaches the lingual half of the talonid. The m2 talonid is unbasined and the region lingual to the hypoconid is more concave than in m1. The cingulid is developed buccally.

Comparisons and discussion (fig. 4N–U, table 6): The lower carnassial has been recovered from the same lignite zone (K1) as the holotype of *Maemohcyon potisati* (Peigné et al., 2006) and is of similar size and morphology. The m2 comes from the Q lignite zone, which is only slightly older (Benammi et al., 2002; Coster et al., 2010; fig. 1). We consider the morphological differences between the holotype and these specimens (i.e., less tapered m1 and m2 talonids, crenulated and curved m1 entoconid crest, more oblique m1 cristid obliqua in the new material) as part of the intraspecific variation recognized within amphicyonid species (e.g., *Amphicyon giganteus* in Ginsburg and Telles Antunes, 1968). This new assessment of the morphological variation in *Maemohcyon* implies that m2 shape is not a useful character differentiating *Maemohcyon* from *Cynelos* (cf. the differential diagnosis of Peigné et al., 2006). In addition, contrary to the initial comparisons of Peigné et al. (2006), the distal transverse reduction of the m2 talonid can no longer be used to differentiate *Maemohcyon potisati* from several *Amphicyon* species: *A. palaeindicus* from the middle and late Miocene of the Potwar Plateau, northern Pakistan (Lydekker, 1876, 1884; Matthew, 1929; Pilgrim, 1932; Colbert, 1935), the middle Miocene Dang Valley, western Nepal (West et al., 1978), and the late Miocene of Yuanmou, southern China (Qi, 2006), *A. shahbazi* from the Oligo-Miocene deposits of the Bugti Hills and the early Miocene Murree Formation in Pakistan (Pilgrim, 1912; Matthew, 1929; Pilgrim, 1932; Ginsburg and Welcomme, 2002), *A. sindiensis* from the middle Miocene basal beds of the Manchar Formation, Sindh Province of southern Pakistan (Lydekker, 1884; Pilgrim, 1932; Raza et al., 1984), and *A. ulungurensis* from the Halamagai Formation of the Junggar Basin, Xinjiang Autonomous Region of China (Qi, 1989; Jiangzuo et al., 2018).

Since the first description of *Maemohcyon* by Peigné et al. (2006), other amphicyonines have been described and are compared here. Specimens of *Amphicyon* sp. are reported from the late Miocene Lower and Upper Irrawaddy formations of Myanmar (Takai et al., 2006; Sein and Thein, 2011). Among these specimens, the material from Tebingan, Magway region of central Myanmar, is a right mandible bearing m1–m2 (Sein and Thein, 2011). Compared with this specimen, *Maemohcyon potisati* exhibits smaller dental dimensions and a more vertical mesial face of the m1 paraconid. Another *Amphicyon* species, *A. zhanxiangi*, has been recently described from the lower part of the Zhang'enbao Formation, in Yehuliquanzigou, and from an unknown locality in Tongxin County, Ningxia Autonomous Region of northern China (Jiangzuo et al., 2019). The material belongs to the late Shanwangian Dingjiaergou local fauna (late early Miocene to early middle Miocene). It comprises an m1 trigonid and a partial maxilla with P4–M3. The morphology of the m1 fragment of *A. zhanxiangi* is rather common for an amphicyonine and does not allow relevant comparisons with *Maemohcyon*. The Chinese species is, however, a larger form, with a width across the protoconid equal to 17.12 mm, according to Jiangzuo et al. (2019), while the m1 width of *Maemohcyon* is 12.3 mm for the holotype and 13.4 mm for the new specimen described here. Moreover, Jiangzuo et al. (2018) described several species of amphicyonids from the middle Miocene Halamagai Formation, northwestern China, including lower molars of the amphicyonines *Cynelos* cf. *bohemicus* and *Amphicyon* cf. *ulungurensis*. Peigné et al. (2006) already noted relevant differences between *Maemohcyon* and *Cynelos* genera, and between *Maemohcyon potisati* and *A. ulungurensis*. Lastly, *Ysengrinia* sp.

TABLE 6. Dental measurements (lower and upper teeth) of *Maemohcyon potisati* and Asian amphicyonines (in mm). Personal measurements and from [a]Pilgrim 1932, [b]Qiu et al. 1986, [c]Kohno 1997, [d]Kordikova 2001, [e]Ginsburg and Welcomme 2002, [f]Qi 2006, [g]Takai et al. 2006 (estimated from the figure), [h]Peigné et al. 2006, [i]Seit and Thein 2011, [j]Jiangzuo et al. 2018, [k]Jiangzuo et al. 2019. * identifies estimates or broken material (MM-40).

	p4	**m1**	**m2**	**M1**	**M2**
Maemohcyon potisati					
TF 2610 (holotype)[h]	16.8×7.7	27.4×12.3	20.3×13.6		
MM-38			23.06×15.5		
MM-39		26.7×13.4			
?Maemohcyon potisati					
MM-40				16.9*×18.5*	
MM-77					16.3×22.8
Amphicyon sp.					
YUDG-Mge 097[i]		32.4×16–18.6	25.1×17.3–17		
unnumbered maxilla[g]				22.4*×28*	19.2*×26*
A. palaeindicus					
GSI D 26 (holotype)[a]					19.3×28.2
PDYV1090[f]					20×29.5
A. pithecophilus					
GSI D 129 (holotype)[a]					19.6×31.7
A. cf. *pithecophilus*					
GSI D 155[a]				27.9×36.3	
A. shahbazi					
PAK 2424[e]					19.3×25
A. cf. *shahbazi*					
GSI D 113[a]				28*×34.5	
Arctamphicyon lydekkeri					
GSI D 133 (holotype)[a]					21.3×30.8
GSI D 134[a]					18.7×27
Askazansoria mavrini					
KE-Ask95-1/4 (holotype)[d]				21.9×29.7	11×22
Ysengrinia sp.					

TABLE 6 *continued*

	p4	m1	m2	M1	M2
HNM-F00002[c]				21.6×26.2	
IVPP V8117[b]		31.6×16	17.2×8.5	22.5×27.9	15.2×22.3
Amphicyon zhanxiangi					
IVPP V24898 (holotype)[k]				25.06×29.22	21.22×28
Cynelos cf. *bohemicus*					
IVPP V24477[j]			16.22×10.84		
Cynelos aff. *helbingi*					
IVPP V24473[j]				17.56×20.58	
IVPP V24474[j]					11.42×16.32

has been reported from the early Miocene Shanwang Basin, Shandong Province of eastern China (Qiu and Qiu, 2013). Previously described as a new unnamed genus of Thaumastocyoninae (Qiu et al., 1986: 24, figs. 1–2), the Chinese form, represented by isolated lower m1 and m2 and a maxilla, has been reassigned to *Ysengrinia*. On both lower molars, only the m1 is illustrated (Qiu et al., 1986: 24, fig. 2) and shows a less vertical mesial face of the paraconid, a more centrally placed protoconid, a higher metaconid, and a shorter talonid as compared to *Maemohcyon*. The description of the m2 does not allow more useful comparisons with *Maemohcyon*. *Maemohcyon* has a longer m1 and shorter m2 than this Chinese form.

Peigné et al. (2006) provide more comparisons with North American, European and African amphicyonines (i.e., *Cynelos*, *Amphicyon*, *Ysengrinia*, *Pseudocyon*, *Ictiocyon*, *Pseudarctos*, *Pliocyon*, *Ischyrocyon*, *Afrocyon* and *Myacyon*), although they were not able to suggest a contemporaneous close relative to *Maemohcyon*. Due to the poor state of preservation and fragmentary nature of Asian amphicyonid fossils (notably in China and Pakistan), most of the remains are attributed by default to the genus *Amphicyon*. Peigné et al. (2006) distinguished the Mae Moh amphicyonid from *Amphicyon* lineages notably because of the nearly vertical buccal faces of the lower teeth (see Peigné et al., 2006 for more comparative details).

?*Maemohcyon potisati* Peigné et al., 2006

Figure 4, table 6

Material: MM-40, right M1 lacking its buccalmost part, MM-77, right M2; both stored at PALEVOPRIM, Poitiers (France).

Description (fig. 4V–W, table 6)*:* Only the lingual part of the right M1 is preserved, bearing the protocone, the pre- and postprotocristae and the lingual cingulum. The mesial and distal borders are roughly parallel; only the buccalmost part of the distal border is gently concave. The preprotocrista is higher than the postprotocrista. The protocone is located slightly

mesially relative to the mesiodistal axis of the tooth. The cingulum surrounds the lingual border symmetrically. A broad, flat, and oblique valley separates the protocone region from the lingual cingulum.

The M2 has a shorter lingual border relative to the buccal one and its distal border is concave. This tooth shows a higher and wider paracone than the metacone. The crest connecting the paracone and metacone creates a shallow but wide U-shaped valley. The buccal cingulum bears a small parastyle at the mesiobuccal base of the paracone. Between the distobuccal face of the paracone and the mesiobuccal face of the metacone, there is a small shelf separating both cusps from the buccal cingulum, where a metastyle is located. A short crest extends down from the metacone tip distolingually, then slightly mesiolingually, where the tiny metaconule rises. The protocone is situated in the midregion of the tooth, mesiodistally, and is closer to the lingual cingulum than to the paracone and metacone. The metaconule and protocone are not connected. The postprotocrista is short and extends only to a very low and small cusp just distobuccal to the protocone. The preprotocrista is long and splits into two crests at the base of the paracone: one crest reaches the middle of the paracone lingual face, the other one, slightly crenulated, extends around the paracone to the middle of its mesial base. There is no paraconule. The lingual cingulum is thicker than the buccal one and extends from the level of the metaconule to the middle of the mesiobuccal crest extending from the preprotocrista. Its thickest part is distolingual to the protocone and its edge is slightly crenulated.

Comparisons (table 6): These upper molars correspond in morphology and size to *Maemohcyon potisati*. We here compare this material to the remains of Miocene Asian amphicyonines.

The only upper dentition material of Miocene amphicyonines recovered in Southeast Asia belongs to *Amphicyon* sp., from the late Miocene Upper Irrawaddy Formation of Myanmar, near Magway (Takai et al., 2006). MM-40 differs from the M1 of the maxilla fragment of this species by having a wider valley between the protocone and the lingual cingulum, and a postprotocrista that is not connected to the lingual cingulum. MM-77 differs from the M2 in being shorter lingually, and in having a more-developed metacone, a less-marked postprotocrista, and a thicker lingual cingulum. The upper molars from Mae Moh are also smaller than in the Magway specimen as estimated from the figure (Takai et al., 2006: fig. 7).

Several species from the Siwaliks have been created based on isolated upper teeth. This is the case of *Amphicyon palaeindicus*, which was first reported from Kushalghar, Punjab Province of northern Pakistan from a single M2 (Lydekker, 1876). The holotype (GSI D 26) is an M2, illustrations of which appearing divergent according to publications (figured by Lydekker, 1876: pl. VII, fig. 5; Lydekker, 1884: pl. XXXII, fig. 8; Matthew, 1929: 482, fig. 19 right). Compared with the holotype cast BMNH M 1558, we observed that MM-77 has a smaller breadth relative to its length, and a metastyle is present. Another M2 is reported from the late Miocene of Yuanmou, in the Yunnan Province of China (Qi, 2006). However, this tooth (PDYV1090, Qi, 2006: 149, figs. 3.16.1a–c) does not resemble the holotype of *A. palaeindicus,* and could belong to a different species of amphicyonid. Compared with this specimen, MM-77 is more asymmetrical, with a less-developed metacone and postprotocrista, and the tooth bears a metastyle

on the buccal cingulum, unlike the Yunnan M2. MM-77 is much smaller than these two specimens from China and Pakistan.

Amphicyon pithecophilus is known from the middle Miocene Chinji Formation of northern Pakistan and from an indeterminate stratigraphic level in the locality of Nurpur, Himachal Pradesh of India (Lydekker, 1884; Pilgrim, 1932). The M2 of ?*Maemohcyon potisati* differs from the M2 of *A. pithecophilus* (holotype GSI D 129, Pilgrim, 1932: pl. II, figs. 3–3a) in being much shorter lingually relative to the buccal side, in having a poorly marked postprotocrista, and in lacking a ridge extending down buccally from the protocone tip. MM-40 differs from the M1 of *A.* cf. *pithecophilus* (GSI D 155, Pilgrim, 1932: pl. II, figs. 2–2a) in having a rounded, not triangular, lingual outline, a more internal and less mesially placed protocone, and uncrenulated pre- and postprotocristae. The upper molars from Mae Moh also have smaller proportions compared with those of *A. pithecophilus*.

Arctamphicyon lydekkeri is reported from the late Miocene Dhok Pathan Formation near Padhri, in the Punjab Province of northern Pakistan (Pilgrim, 1910). The holotype (GSI D 133) is an M2 according to Matthew (1929: 482, fig. 18 left). Pilgrim (1932) identified this tooth as an M1 (Pilgrim, 1932: pl. II, fig. 7) because he described an additional M2 (GSI D 134, paratype, Pilgrim, 1932: pl. II, figs. 8–8a) which probably came from the same spot, and showed "identical colour and state of fossilisation" but a different wear stage (Pilgrim, 1932: 25). For Pilgrim, this could indicate a more distal position of this tooth through the dental row as compared to the holotype. However, Peigné et al. (2006) argued that the differences in dimensions and morphology between these specimens were not sufficient to justify the attribution of the material to a first and second molar, and in consequence, they both are M2s. MM-77 differs from the holotype and the paratype of *Arctamphicyon lydekkeri* by being smaller, lingually narrower, and by having a thicker lingual cingulum, a lower paracone and a metastyle on the buccal cingulum.

Amphicyon shahbazi was initially described from lower dentition from the Oligocene-Miocene deposits of the Bugti Hills, Balochistan Province of Pakistan (Pilgrim, 1912). Later, Pilgrim (1932) described two additional upper dentition specimens from the Bugti Hills, including an upper molar. MM-40 differs from the M1 of *A.* cf. *shahbazi* (GSI D 113, Pilgrim, 1932: pl. II, figs. 6–6a) by being smaller and by showing a more symmetrical morphology and a longer valley between the protocone and the lingual cingulum. Ginsburg and Welcomme (2002) also reported an M2 of *A. shahbazi* (PAK 2424) from the same region. MM-77 differs from it by having a metastyle on the buccal cingulum and a shorter postprotocrista, and by being smaller and shorter relative to its breadth.

Upper molars of Amphicyoninae from the Miocene of Kazakhstan (Bonis et al., 1997; Kordikova, 2001), Japan (Kohno, 1997) and China (Qiu and Qiu, 2013; Jiangzuo et al., 2018, 2019) can also be compared here. *Askazansoria mavrini* from the early Miocene of Askazansor Formation, Betpakdala Steppes of southern Kazakhstan, initially attributed to *Ysengrinia* (Bonis et al., 1997), is represented by a maxilla bearing P4–M2. MM-40 differs from the M1 by bearing more mesially placed protocone and preprotocrista. MM-77 differs from the M2 by being larger and by having a less-reduced metacone and a different tooth outline, with a narrower and more-

rounded lingual border. *Ysengrinia* sp. is recorded by an M1 from the early middle Miocene Korematsu Formation of Shobara, Hiroshima Prefecture of southwestern Japan (Kohno, 1997). The M1 of ?*Maemohcyon potisati* differs from that specimen in having a more symmetrical lingual cingulum. As mentioned before, *Ysengrinia* sp. also occurs in the early Miocene Shanwang Basin, Shandong Province of eastern China (Qiu and Qiu, 2013). On the maxilla bearing P4–M3, the M1 lingual part of this Chinese form is not sufficiently well preserved to allow comparisons with MM-40. However, MM-77 differs from the M2 in having a narrower lingual border relative to the buccal one, a longer preprotocrista subdivided into two crests when approaching the paracone, a postprotocrista developed distolingually and not just distally, and in the presence of a metastyle on the buccal cingulum. Jiangzuo et al. (2018) described several species of amphicyonids from the middle Miocene Halamagai Formation of the Junggar Basin, northwestern China, including upper molars of *Cynelos* aff. *helbingi*. The upper molars of *Maemohcyon* are larger than those of this Chinese form, and their protocones are more centrally placed. Compared with the M2 of *Cynelos* aff. *helbingi*, MM-77 is longer relative to its width, it has a more prominent paracone, a metastyle on the buccal cingulum, a shorter postprotocrista, and a lingual cingulum bending distally. Lastly, *Amphicyon zhanxiangi*, from the early-middle Miocene of Tongxin County, northern China (Jiangzuo et al., 2019), is represented by two specimens including a maxillary fragment with P4–M3, chosen as the holotype of the species. MM-40 differs from the M1 of *A. zhanxiangi* in being more symmetrical. MM-77 differs from the M2 of this species in being triangular rather than rectangular in shape, with a lingual cingulum thickening distally, a prominent paracone, a more-elongated preprotocrista, a poorly distinct postprotocrista and a metaconule. The tooth from Mae Moh is also smaller and shorter relative to its width.

Pseudarctos Schlosser, 1899

cf. *Pseudarctos* sp.

Figure 4

Material: MM-41, left M1; stored at PALEVOPRIM, Poitiers (France).

Description (fig. 4X): MM-41 is relatively symmetric and slightly compressed mesiodistally relative to its breadth, recalling M1 rather than M2 amphicyonid morphology. It is subtriangular and wider than long (L = 8.3 mm, W = 11.9 mm). The lingual root and one of the buccal ones are partially preserved. The lingual root is larger than the buccal one. The paracone and metacone are crestiform and relatively low. The paracone is clearly higher and slightly longer than the metacone. The crest joining these two buccal cusps is marked by a shallow V-shaped notch. The buccal rim displays a developed constriction between the paracone and metacone. The protocone and the pre- and postprotocristae are worn. The protocone is located slightly mesially with respect to the mesiodistal axis of the tooth, the preprotocrista being shorter than the postprotocrista. No conules are visible. The protocone is separated from the lingual cingulum by a narrow valley. Both the protocone and the lingual cingulum are very low. The cingulum is also slightly marked buccally.

Comparisons (fig. 4W): This specimen belongs to a very small amphicyonid species. In the Miocene of Asia, undescribed specimens listed as cf. *Amphicyon* sp. from the middle Miocene Ban San Klang Basin of northern Thailand and from the early Miocene Basal Manchar Formation (locality 2) at Bhagothoro, near Sehwan, Sindh Province of southern Pakistan (Raza et al., 1984; Ducrocq et al., 1995) display the closest similarity in morphology and size to MM-41 (Grohé, personal obs.). The assignment to the wastebasket genus *Amphicyon* is, however, erroneous. The small size and morphology of these specimens rather recall the Eurasian monospecific genera *Ictiocyon* and *Pseudarctos* (Ginsburg, 1992).

Ictiocyon socialis is known from the early Miocene of Europe (MN3–MN4a). In Asia, the species is reported from a mandible coming from the early Miocene beds of the Xianshuihe Formation of Lanzhou Basin, Gansu Province of China (Wang et al., 2005). The larger tooth proportions (M1 L = 9.6 mm, W = 14 mm, MNHN Ar 2554 in Ginsburg, 1992) and the squarer morphology of M1 in *I. socialis* (Ginsburg, 1992) differ notably from the Mae Moh specimen.

Pseudarctos was initially reported in the form of the species *P. bavaricus* from the early and middle Miocene of Europe (MN4–MN9). According to Ginsburg (1992), *P. bavaricus* represents an anagenetic lineage composed of three subspecies, among which size progressively increases through time: *P. bavaricus beaucensis* from the early Miocene (MN4b), *P. bavaricus pontignensis* from the early and middle Miocene (MN5), and *P. bavaricus bavaricus* from the middle and late Miocene (MN6–MN9). This last subspecies is also described from the late Miocene of Yuanmou, Yunnan Province of China (Qi, 2006), but upper molars are only known from Europe. According to the diagnosis of *P. bavaricus bavaricus* provided by Ginsburg (1992), the M1 buccal cusps are low, which could correspond to the morphology observed in MM-41. The subtriangular outline of the Mae Moh specimen associated with a marked constriction between the paracone and metacone are different from the specimens of *P. bavaricus pontignensis* and reminiscent of those of *P. bavaricus beaucensis* figured by Ginsburg (1992). A second occurrence of the genus is reported from the middle Miocene upper bed of Aletexire locality of Tunggur Basin, Inner Mongolia (China) with *Pseudarctos* sp. (Wang et al., 2003). This material is not figured and cannot be compared here. Until additional specimens are found, we attribute the single upper tooth of Mae Moh to cf. *Pseudarctos* sp.

Suborder Feliformia Kretzoi, 1945

Family Viverridae Gray, 1821

Subfamily Paradoxurinae Gray, 1964

***Siamictis carbonensis*,** new genus, new species

Figure 6A–C, table 7

Holotype: MM-45, right mandible with p2–m2 and alveolus of p1; stored at the DMR, Bangkok.

Referred material: MM-43, left mandible with p3–m2 and alveolus of p2; MM-44, left mandible with p2–m1 and alveolus of m2; stored at the DMR, Bangkok.

Etymology: Generic name derived from *Siam*, referring to Thailand, and *ictis*, meaning "marten" in Greek. Species name derived from *carbo*, meaning "coal" in Latin, in reference to the open coal mine of Mae Moh.

Diagnosis: Small Paradoxurinae with low-crowned teeth; diastema between c–p1 and p1–p2; single-rooted p1; developed mesial and distal accessory cuspids on p2–p4; vertical central pillar on the lingual side of the main cuspid preceded and followed by a depression on p2–p4; from p2 to p4, increase of: the separation of the accessory cuspids from the main cuspid, the distal development of the talonid, and the size of the lingual vertical central pillar, becoming an incipient metaconid on p4; p4 with obliquely aligned accessory cuspids and main cuspid, distolingual basined shelf with crenulated border; m1 protoconid higher than paraconid, metaconid smaller and distally placed relative to protoconid, high, equally developed entoconid and hypoconid, hypoconid slightly mesial or directly buccal to entoconid, low distal rim of the talonid with multiple small cuspids, basined talonid; small single-rooted m2, protoconid very buccal, poorly differentiated lingual and distal rims.

Differential diagnosis: Differs from *Mioparadoxurus*, *Kichechia*, *Orangictis*, and *Pseudocivetta* by higher accessory cuspids and molarization of premolars (especially on p4 where an incipient metaconid is present); from *Ketketictis*, *Kichechia*, *Orangictis*, *Tugenictis*, and *Kanuites* by a cristid obliqua parallel to the axis of m1; from *Mioparadoxurus*, *Kichechia*, *Orangictis*, *Tugenictis*, and *Pseudocivetta* by longer trigonid and less lingually positioned paraconid; from *Mioparadoxurus*, *Kichechia*, *Orangictis*, and *Tugenictis* by m2 much shorter relative to m1; from *Kichechia* and *Orangictis* by a lower m2 trigonid and m2 metaconid placed distally relative to the protoconid; from *Mioparadoxurus* and *Pseudocivetta* by a narrower m1 talonid; from *Kichechia* and *Orangictis* by the lack of a cuspid between the metaconid and entoconid; from *Orangictis* by a shallower mandible relative to m1 length; from *Kanuites* by a lower m1 protoconid.

Description (fig. 6A–C, table 7): MM-45 is the best-preserved specimen. The mandible is long and thin. It widens and becomes deeper from the level of p1 alveolus to the level of p4–m1. Behind the m2 and rostrally to the broken angular process, the ventral part of the mandible is concave. The masseteric fossa is relatively deep and its rostral edge reaches below the m2 distal end. The ascending ramus does not rise abruptly distal to m2. Two mental foramina are present on the buccal side: one beneath p1–p2 and another one beneath p3. The lingual mandibular foramen is located far from the dental row (8.8 mm behind). At the rostral end, the symphysis extends to the level of p2. The position of the p1 alveolus reveals two diastemata, between c–p1 and p1–p2. The premolars are asymmetrical. They have mesial and distal accessory cuspids, the positions and proportions of which vary from p2 to p4: the mesial accessory cuspid moves away from the main cuspid by becoming longer and wider, and is shifted lingually to the main cuspid, resulting in a distobuccal alignment of the accessory and main cuspids on p4; the distal accessory cuspids also become lower, further separated from the main cuspid, and displaced buccally relative to the main cuspid tip; the distal cingulid broadens distally and lingually to create a small basin with crenulated borders on p3. This basin is even more developed on p4. A vertical central pillar runs along the lingual face of the main cuspid on p2 and p3. It is preceded mesially by a small depression and distally joins the lingual border

TABLE 7. Dental measurements of *Siamictis carbonensis*, n. gen., n. sp., and selected viverrids including fossil paradoxurines (in mm). Personal measurements and from [a]Pilgrim, 1932, [b]Savage, 1965, [c]Prasad, 1968, [d]Petter, 1973, [e]Morales et al., 2001, [f]Qiu, 2004, [g]Morales and Pickford, 2005, [h]Morlo et al., 2007, [i]Morales and Ginsburg, 2008, [j]Morales and Pickford, 2011, [k]Adrian et al., 2018, [l]Werdelin and Lewis, 2013, [m]Werdelin, 2019. * Estimated.

	c	p1	p2	p3	p4	m1	m2	m2 L/m1 L
Siamictis carbonensis								
MM-45 (holotype)			4.4×1.6	4.9×2	5.3×2.6	6.7×3.5	3.1×3	0.46
MM-43				5.1×2	5.4×2.5	6.5×3.6	3.2×3.1	0.49
MM-44			4.8×2	5×2.4	5.9×2.9	7.2×4.1		
Lufengictis peii								
IVPP V8130-2 (holotype)[f]						12.5×8.5		
IVPP V8130-3 (holotype)[f]							9×6.8	
IVPP V8130-4 (holotype)[f]						11×7.8	8×6.3	0.73
IVPP V8130-5[f]						11.2×7.2		
IVPP V8130-6[f]						11.3×7.7		
Mioparadoxurus meini								
GSI K 29-469 (holotype)[j]				9×5	11.5×6.5	16×10		
Vishnuictis salmontanus								
GSI D 160 (holotype)[a]						10.4*×?	5×?	0.48
Vishnuictis hariensis								
GSI 18080 (holotype)[c]		3×1.5	5×3	6.5×3	8.5×3.5			
Vishnuictis africana								
BAR 280′02 (holotype)[i]					8.8×3.3	9.2×4.4		
Viverra (?) *chinjiensis*								
GSI D 214 (holotype)[a]	5.3×3.5	3×1.5	6.5×2.5		7.5×4	10×5.2	5.7×4.5	0.57
Viverra nagrii								
GSI 18076 (holotype)[c]		2.5×2	5×2.6	6×3	6.5×3			
"Large viverrid" *hasnoti*								
GSI D 135 (holotype)[a]					11.2×5.5	14.5×7.5		
Ketketictis solida								
DPC 5982 (holotype)[h]						9.4×5.2		
Kichechia savagei								

TABLE 7 *continued*

	c	p1	p2	p3	p4	m1	m2	m2 L/m1 L
KNM-MO24 (holotype)[l]			3.4×1.9	4.1×2.4	5.1×2.8	5.6×3.6		
KNM-RU2904l[l]				3.9×2.1	4.2×2.6	5.6×3.1		
KNM-MO17118[l]						6.3×3.6	3.9×3	0.62
Kichechia zamanae								
BMNH M19078 (holotype)[b]				3.6×2.4	4.4×2.9	5.8×3.4		
KNM-RU2922[l]				4.6×2.5	5.6×2.5	6.5×3.4		
KNM-RU2907[l]				3.6×2	4.6×2.7	5.6×3.1		
Orangictis gariepensis								
AD 613′98 (holotype)[e]			5.1×3	6.3×3.9	7×4.4	8.5*×5	5.2×4.1	0.61
AD 119′98 (paratype)[e]	6×4.7		5.1×2.9	6×3.5	7.4×4.5	9.9×5.8		
AD 421′97[e]			4.8×2.7	5.5×3.5	7.1×4.5	9.2*×5.8		
Tugenictis ngororaensis								
BAR 2065′05 (holotype)[g]						12.9×7.6		
BAR 35′98[g]							9×6.3	
Pseudocivetta ingens								
FLK-N 758[d]		7.6×?			19.5×8			
FLK-N 840[d]							11.5×10	
ER 2314[k]						11.9×12.9		
OMO 75/Sd-1970-386						20.8×10.8		
OMO 33-1969-354						21.1×11.7		
Kanuites lewisae								
KNM-LT 3876[m]						8.1×4.1		
KNM-LT 3369[m]						8.3×3.9		
KNM-LT 15093[m]						7.5×3.7		
KNM-FT 3370[m]						6.7×3.8		

of the distal basined shelf. This pillar is more developed on p4 and becomes an incipient metaconid. Together with the main cuspid and the mesial accessory cuspid, it forms a small trigonid. The main cuspids of p2–p4 are approximately as high as the m1 paraconid. The m1 trigonid is rather low-crowned. It is slightly longer and wider than the talonid. The paraconid tip is as lingually located as the metaconid tip. The protoconid is higher than the paraconid. The metaconid is lower than the paraconid (unworn metaconid on MM-44) and is displaced distally with respect to the protoconid, resulting in a lingually opened trigonid. The talonid is well-basined and bears high and equally developed entoconid and hypoconid. Depending on the

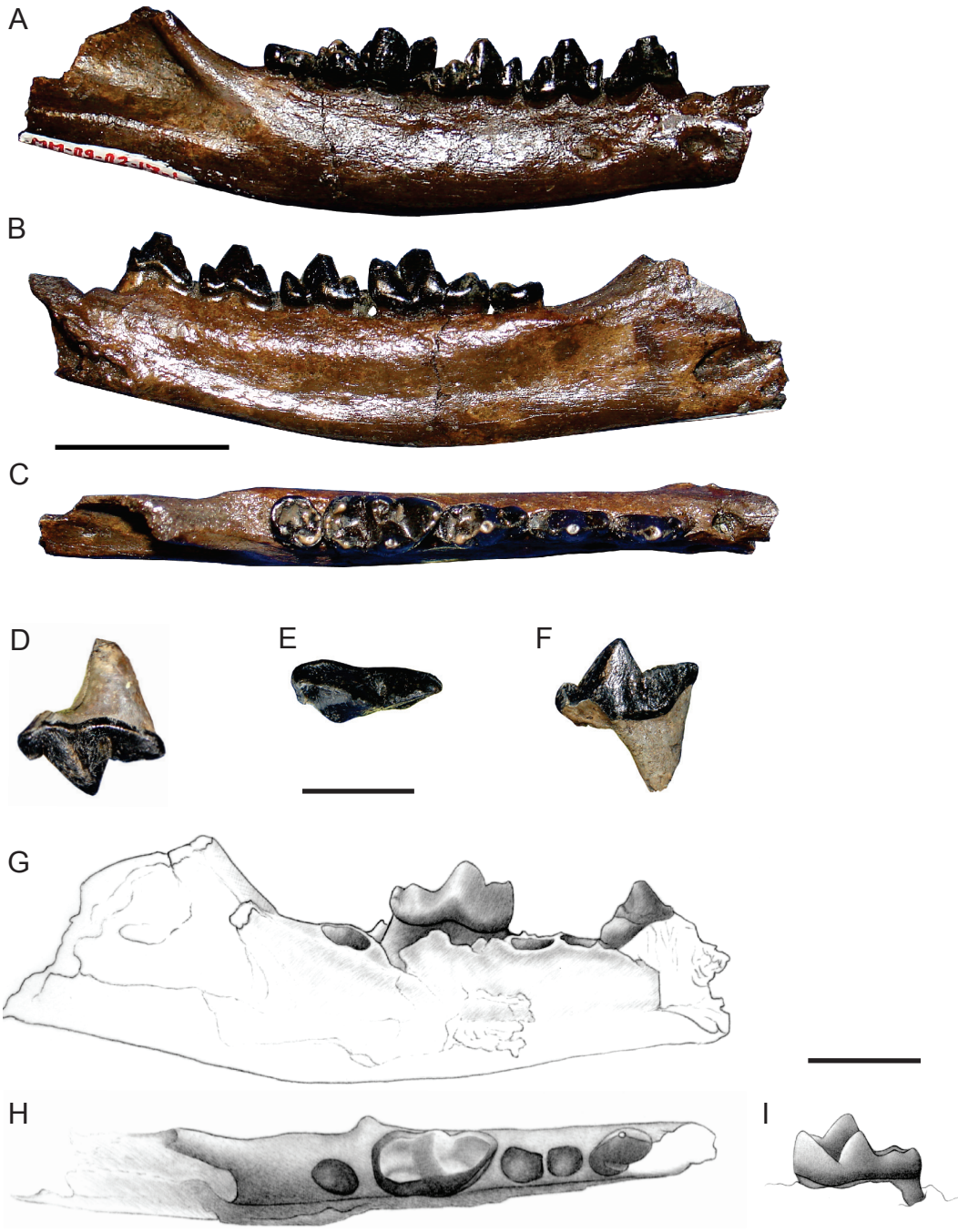

FIGURE 6. *Siamictis carbonensis,* n. gen., n. sp.: **A,** buccal, **B,** lingual, and **C,** occlusal views of the right mandible MM-45, holotype. Feliformia indet.: **D,** buccal, **E,** occlusal, **F,** lingual views of P4, MM-42. cf. *Viverra* sp.: **G,** buccal and **H,** occlusal views of the left mandible TF 2659; **I,** focus on the lingual view of m1 of TF 2659. Drawings by Sabine Riffaut. Scale = 1 cm for A–C, D–F and G–I.

specimens, the hypoconid is shifted mesially with respect to the entoconid (in MM-45) or is directly buccal to it (in MM-43). Between the two cuspids, multiple small cuspids shape the distal rim of the talonid. They are half the height of the entoconid and hypoconid. The m2 is single-rooted and rounded. It bears a reduced paraconid, a high protoconid, and a lower hypoconid. The protoconid is displaced buccally relative to the hypoconid. A lower crest without differentiated cuspids surrounds the lingual and distal rims of the tooth. Cingulids are mainly present at the base of the premolars and at the buccal base of the m1 paraconid.

Comparisons and discussion (table 7): Among viverrids, the structure of the lower carnassial (i.e., wide talonid, individualized entoconid and hypoconid) is reminiscent of the hypo- and mesocarnivorous subfamilies Hemigalinae, Paradoxurinae, and Viverrinae. Compared with extant Viverrinae genera (*Civettictis*, *Viverra* and *Viverricula*), *Siamictis*, n. gen., has a narrower and shorter protoconid, resulting in similar proportions of the trigonid and talonid. We thus compared *Siamictis* with non-hypercarnivorous viverrid taxa morphologically close to extant hemigalines and to fossil paradoxurines (Morales and Pickford, 2011; Adrian et al., 2018).

In Asia, two species show morphological similarities with extant hemigalines and paradoxurines. *Lufengictis peii* from the late Miocene of Lufeng, Yunnan Province of China (Qi, 2004), is very similar to the extant *Cynogale bennettii* (otter civet). *Siamictis* differs from *Lufengictis* by having much smaller dimensions, a narrower m1, a longer m1 paraconid, m1 trigonid cuspids higher than the talonid ones (as opposed to similarly low trigonid and talonid in *Lufengictis*), and a much shorter m2 relative to m1. Compared with *Mioparadoxurus meini* from the late Miocene of Haritalyangar, northern India (Morales and Pickford, 2011), *Siamictis* displays much smaller dimensions, much higher accessory cuspids on p4 that is also molarized, a m1 protoconid higher than the p4 main cuspid, a narrower m1 with a longer paraconid, and a talonid as wide as the trigonid (wider than the trigonid in *Mioparadoxurus*).

Several other Miocene viverrid genera with hypo- or mesocarnivorous forms were originally described from the Siwalik Hills of Pakistan and India: *Vishnuictis*, *Viverra*, and an unnamed large viverrid genus (Lydekker, 1884; Pilgrim, 1932; Pilbeam et al., 1979). Three species of *Vishnuictis* are reported from the Miocene-Pliocene of the Indian Subcontinent and China. The type species, *V. durandi*, is represented by two skulls (Lydekker, 1884; Pilgrim, 1932) from uncertain horizons of the Siwaliks, which cannot be compared with *Siamictis* except for their size, which is larger. *V. salmontanus* has been recovered from the late Miocene of the Dhok Pathan Formation of Pakistan and from Yuanmou, Yunnan Province of China (Pilgrim, 1932; Qi et al., 2006; Dong and Qi, 2013). According to the description of Pilgrim (1932: 103), the holotype GSI D 160 shows diastemata between c–p1 and p1–p2, the m1 trigonid is longer than the talonid, the m1 paraconid points lingually, and the m1 metaconid is smaller than the protoconid, as in *Siamictis*. The m2 outline (Pilgrim, 1932: pl. IV, fig. 8a) is, moreover, similar to that in *Siamictis*. However, in *V. salmontanus*, tooth proportions are larger, the m1 protoconid is broader, and the m2 bears two distolingual distinct cuspids. *Vishnuictis hariensis*, known from the Indian late Miocene locality of Haritalyangar (Prasad, 1968), does not show any diastema between p1 and p2, unlike *Siamictis*. A fourth species of this genus, *V. africana*, is recorded in Africa, in the middle Miocene Muruyur Formation of Kipsaraman, Baringo District, Kenya (Morales and Pickford, 2008). *Siamictis* differs

from *V. africana* in its smaller dimensions, the presence of a metaconid ridge on p4, and the lack of an internal cuspid on the m1 talonid basin.

Viverra chinjiensis has been recovered from the middle Miocene of the Chinji Formation (Pilgrim, 1932) and the early late Miocene of the Nagri Formation, northern Pakistan (Pilbeam et al., 1979), as well as from the middle Miocene of Ramnagar (Basu, 2004) and the late Miocene of Kalagarh (Tiwari, 1983; Patnaik, 2013), both in northern India, and from the middle Miocene of Chaungtha, Myanmar (Chavasseau et al., 2013). Morales and Pickford (2008) noted that this species should be provisionally referred to *Vishnuictis*. The only figured material of the species is the holotype, a mandible and an associated upper molar (GSI D 214, Pilgrim, 1932: pl. IV, figs. 9–9a and 10). *Siamictis* differs from *V. chinjiensis* in having smaller dimensions, higher and longer mesial accessory cuspids, a metaconid ridge on premolars (especially on p4), a cristid obliqua parallel to the axis of the tooth rather than distobuccally oriented, m2 cuspids lower than the m1 talonid ones, a more mesially placed protoconid on m2, and a shorter m2 relative to m1.

Viverra nagrii is described by Prasad (1968) on the basis of mandible fragments from the late Miocene of Haritalyangar. *Siamictis* differs from the holotype of *V. nagrii* (GSI 18076, Prasad, 1968: pl. IV, fig. 5) by having much higher mesial accessory cuspids and more-developed distal ones.

Lutrinae gen. indet. *hasnoti* (= "large, probably new viverrid genus" according to Pilbeam et al., 1979) is known from the late Miocene of the Nagri and Dhok Pathan formations of northern Pakistan (Pilgrim, 1932; Pilbeam et al., 1979). *Siamictis* differs from the holotype of this species (GSI D 135, Pilgrim 1932: pl. II, figs. 18, 18a, 18b) in having much smaller dimensions, a p4 with a metaconid ridge, a much higher mesial accessory cuspid and a more buccally placed distal one so that the distal shelf is developed lingually to the distal accessory cuspid (and not both lingually and buccally to it as in the Pakistani viverrid), and an m1 with a broader talonid and a narrower protoconid.

Outside Asia, the meso- and hypocarnivorous fossil viverrids are mainly restricted to Africa, with six genera attributed to the paradoxurine subfamily: *Ketketictis*, *Kichechia*, *Orangictis*, *Tugenictis*, *Pseudocivetta*, and *Kanuites* (Morales and Pickford, 2011; Adrian et al., 2018; Werdelin, 2019). *Ketketictis solida* is represented by an isolated m1 discovered in the early Miocene site of Wadi Moghra (= Wadi Moghara), in Egypt (Morlo et al., 2007). *Siamictis* differs from *Ketketictis* by displaying smaller dimensions, a broader talonid (as wide as the trigonid), higher hypoconid and entoconid, and a lower distal rim of the talonid. *Kichechia* is represented by two species from the early Miocene of Rusinga and Mfwanganu Islands, Songhor, and the Kalodirr Member of the Lothidok Formation of West Turkana, Kenya and possibly Napak, Uganda (Savage, 1965; Werdelin and Peigné, 2010; Adrian et al., 2018). *Siamictis* and *Kichechia* have similar m1s length but the premolars of *Siamictis* are narrower relative to their lengths. Moreover, *Siamictis* differs from *Kichechia* by having well-developed accessory cuspids on premolars, a much higher mesial accessory cuspid and an incipient metaconid on p4, a m1 with a less lingually oriented paraconid, a more distal metaconid, no cuspid between the metaconid and entoconid, a cristid obliqua parallel to the axis of the tooth, a lower m2 trigonid with a

metaconid placed distally relative to the protoconid (opposite condition in *Kichechia*), and a shorter m2 relative to m1. *Orangictis gariepensis* was initially recorded from the middle Miocene of Arrisdrift, southern Namibia (Morales et al., 2001), by several mandibles. Additional isolated lower and upper molars from the middle Miocene of Fort Ternan, western Kenya, are referred to *Orangictis* sp. (Werdelin, 2019). *Siamictis* differs from *Orangictis* by exhibiting smaller dimensions, a tendency to the molarization of premolars with an incipient metaconid on p4, a shallower mandible relative to m1 length, narrower premolars relative to their lengths, a longer m1 paraconid, lack of a small cuspid between the m1 entoconid and metaconid, a cristid obliqua parallel to the axis of the tooth on m1, a shorter m2 relative to m1, m2 cuspids lower than those of the m1 talonid, and an m2 metaconid placed distally relative to the protoconid (opposite to the condition in *Orangictis*). *Tugenictis ngororaensis* remains come from sediments of the middle Miocene Ngorora Formation exposed in western Kenya (Morales and Pickford, 2005). This species is known by only two isolated lower molars of much larger dimensions compared with *Siamictis*. Relative to *Tugenictis*, the m1 of *Siamictis* displays a longer paraconid, a more distal metaconid, much lower talonid cuspids, and a cristid obliqua parallel to the axis of the tooth. Even if the m2 of *Tugenictis* does not belong to the same individual as the m1, it was certainly longer relative to m1 as compared to *Siamictis* (calculated m2/m1 L = 0.7 from the measurements of Morales and Pickford (2005) compared with 0.4–0.5 in *Siamictis*). *Pseudocivetta ingens* has been recovered from the early Pleistocene of the Shungura and Koobi Fora formations, in the Omo-Turkana basin, from Melka Kunture in Ethiopia, and from Olduvai in Tanzania (Petter, 1967, 1973; Petter and Howell, 1977; Geraads et al., 2004; Werdelin and Lewis, 2013). It is a much larger form as compared to *Siamictis*. The m1 of *Siamictis* differs from those of *Pseudocivetta* (O 33-354, Petter and Howell, 1977: 284; L39-13, Werdelin and Lewis, 2013: 91, fig. 6.8) by having a higher and longer trigonid and more distal metaconid and entoconid. Moreover, *Siamictis* also differs in p4 morphology by displaying higher cuspids and an incipient metaconid (p4s of *P. ingens*: 758 FLK NNI, Petter, 1973: pl. IV, fig. 12; 768 FLK NNI, Petter and Howell, 1977: 284). *Kanuites lewisae* is recorded in middle Miocene deposits of Fort Ternan, Kenya (Dehghani and Werdelin, 2008; Werdelin, 2019). *Siamictis* differs from *Kanuites* by being slightly smaller and displaying an m1 with a less lingually placed paraconid, a lower protoconid, a cristid obliqua parallel to the axis of the tooth, and multiple small cuspids between the hypoconid and entoconid (instead of a single hypoconulid in *Kanuites*).

Due to the scarcity of material attributed to putative paradoxurines, their phylogenetic relationships and their geographical origin remain unclear. Morales and Pickford (2011) proposed hypotheses of phylogenetic relationships among fossil and extant paradoxurines, placing *Pseudocivetta* and *Mioparadoxurus* as the closest relatives to the extant *Paradoxurus*, while other cladistic analysis by Adrian et al. (2018) and Werdelin (2019) suggested different intergeneric relationships. Regarding viverrid diversity, *Siamictis* is a very small form with a dental morphology close to that of extant paradoxurines. *Siamictis*, however, exhibits a more primitive morphology, with a longer and more-opened trigonid on m1, and less bunodont teeth, and a more-derived morphology of its premolars, with notably high accessory cuspids and an incipient metaconid on p4.

Subfamily Viverrinae Gray, 1964

cf. *Viverra* sp.

Figure 6G–I

Material: TF 2659, right mandible with p3 and m1, and alveoli of p4 and m2; stored at the DMR, Bangkok.

Description (fig. 6G–I): The mandible is partially crushed, and the middle of the horizontal ramus caved in. Its lingual part sits on the sediments. It is also broken at the level of the ascending ramus and mesially to p3. In buccal view, the masseteric fossa is relatively deep and no foramina are visible. The p3 is approximately as high as the m1 paraconid. It bears a very small mesial accessory cuspid. The distal accessory cuspid is weak, merging with the distinct distal crest, and extending down from the main cuspid to about half its height. The distalmost part of p3 is broken off buccally, but indicates that the premolar is wider distally than mesially. Behind p3, the presence of small alveoli suggests a double-rooted p4 (L = 6.8 mm; W = 3.4 mm, estimated measurements), with a mesial root that is smaller than the distal one, and a longer crown length than that of p3. The m1 (L = 10.5 mm; W = 5.3 mm) has a trigonid as wide as and longer than the talonid. The protoconid is higher than the paraconid. The metaconid is slightly lower than the paraconid and half as long as the protoconid. The metaconid tip is slightly distal to the level of the protoconid tip, creating an open trigonid. The talonid is weakly basined. The cristid obliqua is slightly distobuccally oriented. The hypoconid is the highest cuspid of the talonid. The entoconid is displaced slightly mesially relative to the hypoconid. A low hypoconulid is present, distobuccally to the entoconid, at the lingualmost part of the distal border of the talonid. The m2 was single-rooted and small (probably as long as the m1 talonid), as indicated by the alveolus. The mesial edge of m2 alveolus extends mesiobuccally.

Comparisons: This species has a rather wide m1 talonid bearing a well-developed entoconid, and a p4 with a distal accessory cuspid, recalling the morphology of viverrids from the subfamily Viverrinae. It is much larger than *Siamictis* and its dental morphology is very different (e.g., very small mesial accessory cuspid and much smaller distal accessory cuspid on p3, distobuccally oriented cristid obliqua, hypoconid higher than entoconid, and hypoconid displaced distally relative to entoconid). The size and dental morphology rather remind those of *Viverra* spp. (e.g., trigonid cuspids of different height, talonid approximately as wide as the trigonid, three distinct talonid cuspids). Among Asian *Viverra* species, the Thai specimen differs from *V. chinjiensis* Pilgrim, 1932, from the middle to late Miocene of the Siwaliks and Myanmar (Pilbeam et al., 1979; Tiwari, 1983; Basu, 2004; Patnaik, 2013; Chavasseau et al., 2013) by being much larger and having a less distobuccally oriented cristid obliqua, and by a narrower protoconid on m1. It differs from *V. nagrii* Prasad, 1968, from the late Miocene of India, by a reduced distal accessory cuspid on p4. It differs from *V. bakerii* Bose, 1879, possibly from the late Pliocene–early Pleistocene Pinjor Formation of the Siwaliks, by its smaller dimensions (Lydekker, 1884; Pilgrim, 1932). It differs from *V. peii* Qiu, 1980, from the late Pliocene–early Pleistocene of Zhoukoudian, near Beijing, by being much smaller and bearing a narrower

protoconid, a broader and higher metaconid, and a less distobuccally oriented cristid obliqua on m1. Outside Asia, *V. leakeyi* Petter, 1963, is a giant form of civet recorded from the late Miocene to the early Pleistocene in several localities of northern, eastern, and southern Africa (e.g., Petter, 1963; Hendey, 1974; Petter and Howell, 1977; Geraads, 1997; Werdelin, 2003; Werdelin and Peigné, 2010). One of the best-illustrated m1s comes from the Shungura Formation, Omo Basin of Ethiopia, and is figured by Peigné et al. (2008). The Thai viverrine differs from that specimen of *V. leakeyi* by a narrower protoconid, a more mesial entoconid and the lack of an additional cuspid mesial to the entoconid. *Viverra howelli* Rook and Martinez-Navarro, 2004, is recorded from the late Miocene deposits of Bacinello-Cinigiano Basin, in the Grosseto Province of Italy, as well as from Sahabi, in Libya (Howell, 1987) and as well as Lothagam, in Ethiopia (Werdelin, 2003) according to Rook and Martinez-Navarro (2004). The Mae Moh viverrine differs from the holotype of *V. howelli* by a narrower protoconid, a shallower trigonid lingual valley and a more mesial and lower entoconid. Among European fossils, it differs from *Viverra pepratxi* (Depéret, 1890) from the early Pliocene of France by a larger metaconid, the lack of a cuspid at the base of the protoconid, and a more distal hypoconid as compared to the entoconid. In summary, the Mae Moh viverrine could belong to a new species of *Viverra*, but further determination would be premature.

Family Herpestidae Gray, 1964

Leptoplesictis Major, 1903

Type species: *Herpestes filholi* Gaillard, 1899.

Other species included: *L. aurelianensis* (Schlosser, 1888), *L. atavus* Beaumont, 1973, *L. rangwai* Schmidt-Kittler, 1987, *L. mbitensis* Schmidt-Kittler, 1987, *L. senutae* Morales et al., 2008, *L. namibiensis* Morales et al., 2008, *L. peignei*, n. sp.

Diagnosis (from Werdelin and Peigné, 2010: 636):

> Small-sized carnivoran; dental formula (lower dentition only) I 3, C 1, P 4, M 2; premolars with tall cusps; p4 posterior accessory cusp very large; m1 postvallid notch less deep than in *Herpestes*; m2 trigonid and talonid distinct.

Remarks: Major (1903) proposed the name *Leptoplesictis* for *Herpestes filholi* Gaillard, 1899, from La Grive Saint-Alban, Isère, France, because of the slenderness of the teeth relative to the extant genus *Herpestes*. *Herpestes filholi* is *de facto* the type species of the new genus. He also created another species, *Leptoplesictis minor*, based on a small size difference with *L. filholi* (the length of p4–m1 is "21.5 mm in *L. filholi,* against 18 mm in *L. minor*"; Major, 1903: 536). *Leptoplesictis minor* was later synonymized with *L. filholi* by Roth (1988).

Geographical and stratigraphical distribution: Early Miocene of Artenay, France (MN4; Ginsburg, 2002), Petersbuch 2, Germany (MN4; Roth, 1988), Rusinga Island, Kenya (17–15 Ma; Schmidt-Kittler, 1987), Grillental and Langental, Sperrgebiet, Namibia (20–19 Ma; Morales et al., 2018); Middle Miocene of Pontlevoy, France (MN5; Gervais, 1967–1969; Stehlin and Helbing, 1925), Vieux-Collonges, France (MN5; Beaumont, 1973), Sansan, France (MN6;

Ginsburg, 1961; Roth, 1988; Peigné, 2013), Stein am Rhein, Germany (MN6; Roth, 1988), lower Hostalets de Pierola, Spain (MN7/8; Fraile et al., 1997; Morales et al., 1999), La Grive-Saint-Alban, France (MN7/8; Gaillard, 1899); late middle Miocene of Q–K lignite zones of Mae Moh Basin, Thailand (13.4–13.2 Ma; this study).

***Leptoplesictis peignei*,** new species

Figure 7, table 8

Holotype: MM-51, left mandible with p2–m1 and alveolus of p1; stored at the DMR, Bangkok.

Referred material: MM-46, left mandible (p3–m1 with p3 and m1 trigonid broken, alveoli of m2, p2 and p1), stored at the DMR, Bangkok; MM-47, left mandible (p4–m1, alveolus of m2), stored at PALEVOPRIM, Poitiers; MM-48, right mandible (p3–m1 with p4 and m1 trigonid horizontally broken, distal alveolus of p2 and alveolus of m2), stored at PALEVOPRIM, Poitiers; MM-49, right mandible (p3), stored at PALEVOPRIM, Poitiers; MM-50, right mandible (m1, alveolus of m2), stored at PALEVOPRIM, Poitiers; MM-52, right mandible (m1, alveoli of p4 and m2), stored at the DMR, Bangkok; MM-53, right mandible (m1, broken p4 and p3), stored at the DMR, Bangkok; MM-103, left mandible (broken p3, p4, mesial root of m1) and associated lower canine, stored at PALEVOPRIM, Poitiers.

Etymology: Species name in memory of Stéphane Peigné, who greatly contributed to carnivoran systematics and evolution.

Diagnosis: Medium-sized *Leptoplesictis*; m1 with open trigonid and basined tricusped talonid with a dominant hypoconid; single-rooted p1; p2 without accessory cuspids; p3 and p4 with a tiny and a small mesial accessory cuspid, respectively; p3 and p4 with a distal accessory cuspid, very large in the latter.

Differential diagnosis: Differs from *L. filholi*, *L. aurelianensis*, *L. atavus*, *L. mbitensis*, and *L. rangwai* by a larger size; from *L. filholi* by a lower mesial accessory cuspid on p3 and p4, the lack of a basal cingulid mesial to the mesial accessory cuspids, and a relatively shorter m2 (from the alveolus); from *L. aurelianensis* by a shorter m1 trigonid and a longer m2 (from the alveolus); from *L. atavus* by the presence of a distal accessory cuspid on p3, a higher distal accessory cuspid on p4, a more open m1 trigonid with metaconid tip bending backward, and lower entoconid and hypoconid; from *L. rangwai* by a lower mesial accessory cuspid on p4, a higher m1 metaconid, and a shorter m2 (from the alveolus); from *L. mbitensis* by the lack of a lingual cuspid on p4 talonid; from *L. senutae* by a shorter and narrower p2, and the presence of an hypoconulid on the m1 talonid; from *L. namibiensis* by a smaller size, and a lower-crowned m1 talonid.

Description (fig. 7, table 8): The mandible MM-46 preserves the longest ramus in the sample. The ventral border of the specimen is convex from the canine level to m2, and concave at the level of the ascending ramus. The angular process is broken off but its distal end is located at 17 mm from the rostralmost part of the masseteric fossa. In buccal view, the most distal part of the ramus shows a flat triangular surface, just ventral and caudal to a deep masseteric fossa.

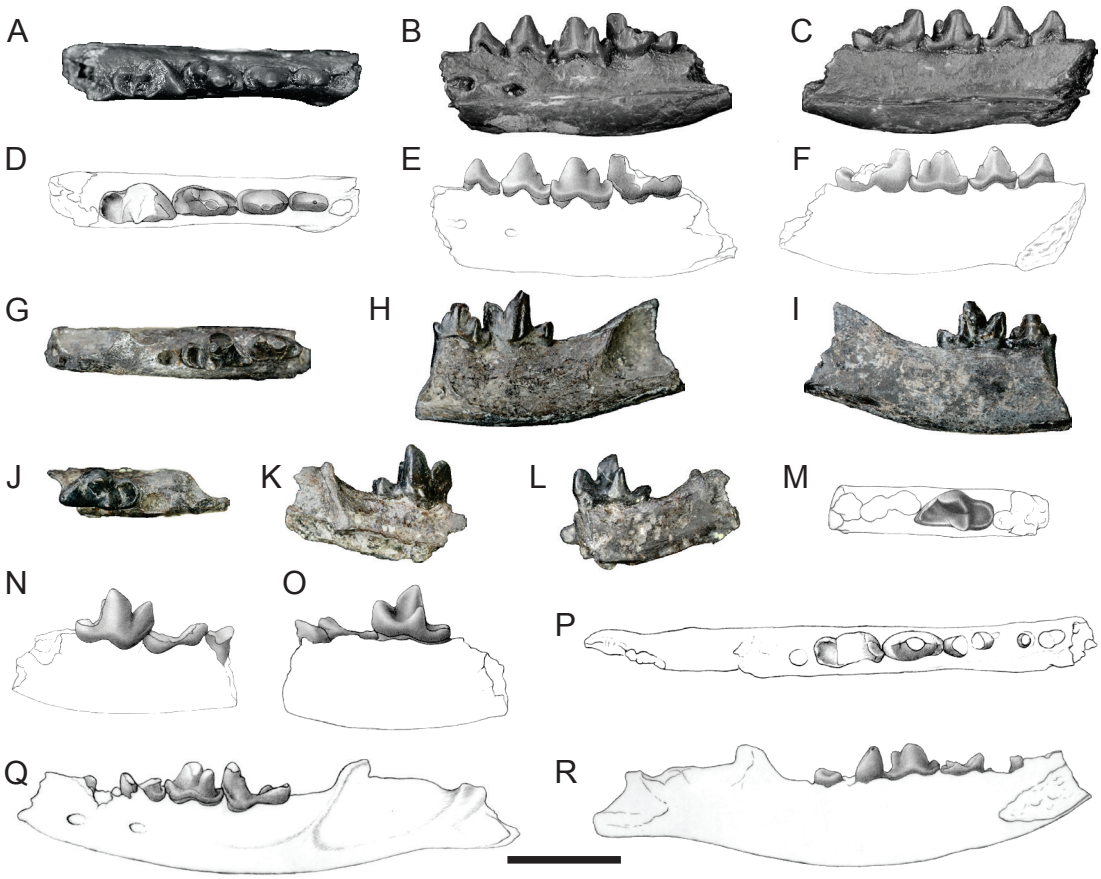

FIGURE 7. *Leptoplesictis peignei,* n. sp.: **A,** occlusal, **B,** buccal, and **C,** lingual views of the cast of the left mandible MM-51, holotype (**D, E, F,** respective drawings); **G,** occlusal, **H,** buccal, and **I,** lingual views of the left mandible MM-47; **J,** occlusal, **K,** buccal, and **L,** lingual views of the right mandible MM-50; **M,** occlusal, **N,** buccal, and **O,** lingual views of the right mandible MM-53; **P,** occlusal, **Q,** buccal, and **R,** lingual views of the left mandible MM-46. Photos by O.C., drawings by Sabine Riffaut. Scale = 1 cm.

In lingual view, the angular process curves lingually to delineate the ventral outline of the medial pterygoid muscle insertion area. The ascending ramus is broken off dorsally, so that the coronoid process and articular condyle are not preserved and the masseteric fossa is not complete. Mental foramina are present under the p1–p2 contact and under p3 (under the midpart of p3 for MM-46 and MM-49 while under the mesial root of p3 for MM-48 and MM-51). The lingual mandibular foramen is located far from the dental row (approximately 8.5 mm behind the distal edge of the m2 alveolus). The mandibular symphysis extends to the distal root of p2. The p1 and m2 are single-rooted. Specimen MM-51 allows observation of more details on the premolars. The p2 is lower than the p3–p4, which have approximately the same height, similar to that of the m1 paraconid. The p2 shows a small distal unbasined shelf, and the main cuspid is displaced mesially relative to the long axis of the tooth. The p3 has a tiny mesial accessory cuspid at the mesial base of the main cuspid, a distal accessory cuspid slightly buccal to the

TABLE 8. Dental measurements (lower teeth) of *Leptoplesictis peignei* n. sp., *Leptoplesictis* species and *Herpestes* (in mm). Personal measurements and from [a]Gaillard, 1899, [b]Petter, 1987 (mean measurements for two *Herpestes* species), [c]Schmidt-Kittler, 1987, [d]Roth, 1988, [e]Morales et al., 2008, [f]Peigné, 2013. * identified estimates or broken material.

	m2	m1	p4	p3	p2	p1	m2 L/ m1 L	m1 W/m1 L
Leptoplesictis peignei								
MM-51 (holotype)		6.5×3.3	5.3×2.4	4.3×1.9	3.1×1.4			0.51
MM-53		7.1×3.5	5.4×?					0.49
MM-46		5.9×?	5.1×2.2	3.9×?				
MM-47		6×3.1	4.9×2.4					0.52
MM-48		6.3×2.7*	5.4×2.2	3.9×1.8				0.43
MM-49				3.9×2.2				
MM-50		7×3.6						0.51
MM-52		6.2×3.1						0.5
MM-103			4.9×2.2					
Leptoplesictis filholi								
MNHN L Gr 1372 (holotype)[a]	2.5×2	5×?	4.5×?	4×?			0.5	
Leptoplesictis aurelianensis								
BSPG 1976 XXII 3669[d]	1.6×1.2	5.6×2.5	4.5×2	3.7×1.4			0.34	0.45
SMNS 44366[d]			4.7×2.1					
Leptoplesictis atavus								
FSL VxC 65580 (holotype)[d]		5.1×2.4						0.47
NHMB Ss 5340[d]		4.7×2.5						0.53
MNHN Sa 940[f]			3.6×1.5	3.3×1.3				
Leptoplesictis mbitensis								
KNM-RU-159994 (holotype)[c]		5.1×2.7	3.9×2.2					0.53
KNM-RU-15991[c]		5.1×2.5						0.49
Leptoplesictis rangwai								
KNM-RU-15990 (holotype) right[c]	2.4×1.9	5×2.7					0.48	0.54
KNM-RU-15990 (holotype) left[c]	2.4×1.9	5.1×2.7	4.1×1.9				0.47	0.53
KNM-RU-2900[c]		4.9×2.7						0.55
KNM-RU-15992[c]		4.9×2.6						0.53

TABLE 8 *continued*

	m2	m1	p4	p3	p2	p1	m2 L/ m1 L	m1 W/m1 L
Leptoplesictis senutae								
GT 1′06[e]		6×3	5×2.5	4.3×2.1	3.4×2	1.5×1.6		0.5
Leptoplesictis namibiensis								
LT 50′07[e]		8.3×4.4						0.53
Herpestes sanguineus[b]	2.66×2.06	5.36×3.03	4.67×2.24				0.49	0.56
Herpestes pulverulentus[b]	3.18×2.36	6.1×3.46	5.45×2.62				0.52	0.57

main cuspid and merging with its distal face (accessory cuspid poorly developed in MM-51, more distinct in MM-49 and even more so in MM-48, although it remains small), and a small cingular shelf oriented distolingually and unbasined. This talonid is marked buccally by a crest and closed lingually by a cingulid. It appears higher at the distal end of the tooth than at the base of the main cuspid distal face. The p4 bears a small mesial accessory cuspid that is more developed than in p3 and bends lingually. It also displays a prominent distal accessory cuspid located midheight to the main cuspid and buccal to its tip, so that the three cuspids of p4 are obliquely aligned. A lingual cingular shelf extends on the distal part of this premolar. This talonid is larger than in p3 and the difference in height between the mesial and distal part of the talonid is even more marked. The m1 has a longer, wider, and higher trigonid than talonid. The protoconid is much higher than the paraconid. The metaconid is slightly lower and narrower than the paraconid in lingual view, and its tip is displaced distally relative to the protoconid tip. The mesial faces of the protoconid and metaconid curve backward. The distal crest of the paraconid and the mesial crest of the metaconid are not connected lingually and a wide and deep trigonid valley opens between these cuspids, well separated from each other. The talonid basin is very low and shallow. The hypoconid is the highest talonid cuspid. A hypoconulid and an entoconid are present on the distal and distolingual borders of the talonid, respectively. The entoconid is slightly distal relative to the hypoconid. The cristid obliqua is poorly oriented distobuccally and reaches mesially the middle of the protoconid distal face. The m2 alveolus is small and approaches the length of the m1 talonid. Cingulids are present at the mesiobuccal base of m1 and on the lingual side of the premolars, at the level of the accessory cuspids and distal shelves.

Comparisons and discussion (table 8): The high trigonid and narrow talonid of m1 in association with a relatively short m2 and accessory cuspids on p3–p4 resemble the morphologies observed in some extant Herpestidae (particularly *Herpestes*). The only herpestid of the Miocene Asian fossil record is the extant genus *Herpestes*. Barry (1983) reported some material from the late Miocene of the Potwar Plateau, in the Punjab Province of Pakistan. Barry (1983) recognized three species of *Herpestes* representing the oldest fossil record of the family in Asia.

Only ?*Herpestes* large species is represented by lower dentition, a mandible with p4 (GSP 217, Barry, 1983: 153, fig. 3). This specimen is much larger than the Mae Moh material and shows a p4 morphology that is relatively typical for viverrids and herpestids (i.e., small mesial accessory cuspid, distobuccal accessory cuspid and distolingual extension of the cingulid into a shelf). Besides, our Thai form differs from *Herpestes* by the talonid borders of m1: the lingual border at the base of the metaconid is higher in the Thai material than in *Herpestes* specimens, so that the lingual and buccal borders of the talonid at the base of the trigonid are of equal height. Moreover, the m1s of our Thai form are also more slender than the m1s of *Herpestes* (index m1 W/m1 L = 0.43 to 0.52 for *Leptoplesictis peignei* against a mean ratio of 0.56 for *Herpestes sanguineus* and 0.57 for *H. pulverulentus* from measurements in Petter, 1987).

Very close to *Herpestes* in morphology, *Leptoplesictis* Major, 1903, includes seven species recovered from early and middle Miocene localities of Europe and Africa. The type species, *L. filholi* (Gaillard, 1899), recorded from the middle Miocene of Europe (MN6–MN7/8; Beaumont, 1973; Roth, 1988; Peigné, 2013, and references therein) is smaller and has a higher and stronger mesial accessory cuspid with a basal cingulid on p3 and p4, and the m2 alveolus is elongated and pear shaped, unlike in our specimens (Gaillard, 1899; Beaumont, 1973). *Leptoplesictis aurelianensis* (Schlosser, 1888) is known from the early and possibly middle Miocene of Europe (MN4–MN5; see Roth, 1988; Peigné, 2013, and references therein). *L. aurelianensis* has similar developments as the Thai form in the accessory cuspids on p3 and p4, the presence of a distolingual talonid on premolars, m1 trigonid wider than talonid and with a distally placed metaconid, and a low talonid with poorly differentiated cuspids. However, this species is smaller than the Thai taxon, the m1 trigonid is more elongated and the m2 is shorter (Roth, 1988). *Leptoplesictis atavus* Beaumont, 1973, from the middle Miocene of Europe (MN5–MN6; Beaumont, 1973; Ginsburg, 1961; Roth, 1988; Peigné, 2013), is a smaller form than the Thai species. The m1 metaconid is straight and less distal (not visible in buccal view). The paraconid and metaconid are therefore close to each other, with the distal crest of the paraconid and the mesial crest of the metaconid forming a narrow V-shaped valley, while those cuspids are more separated from each other and their crests are not connected in the Thai material (Roth, 1988). The talonid cuspids, entoconid and hypoconid, are higher than in *L. aurelianensis* and the Thai form (Roth, 1988). A mandible from Sansan attributed to *L. atavus* by Peigné (2013) allow us to compare the morphology and proportions of its premolars with our taxon: *L. atavus* bears a weaker distal accessory cuspid on p4 relative to the Thai form, the distal accessory cuspid is absent on p3, and this tooth is only slightly shorter than p4, unlike in the Thai form. Four additional species are described from the early Miocene of Africa: two from Rusinga Island, Kenya (Schmidt-Kittler, 1987), and two from Sperrgebiet, Namibia (Morales et al., 2008). The holotype of the Kenyan species *L. rangwai* shows a p4 with a considerably higher mesial accessory cuspid, approximating the height of the distal one, a lower metaconid on m1, and a relatively longer m2 as compared to the Thai species (Schmidt-Kittler, 1987). Most cuspids of p4 and m1, such as the distal accessory cuspid of p4, appear somewhat bulbous, which is different from the sharp tooth morphology of the Thai species. The second Kenyan species, *L. mbitensis*, differs from *L. rangwai* and from the Thai species by having a lingual cuspid on its p4 distal shelf (Schmidt-Kittler, 1987). Our form differs from

L. senutae from Grillental (Morales et al., 2008) by a shorter and narrower p2 and by the presence of a hypoconulid on the m1 talonid. It differs from *L. namibiensis* from Langental (Morales et al., 2008) by its smaller size and by the presence of a lower-crowned m1 talonid. Our Thai form therefore pertains to a new species of *Leptoplesictis*, and represents the earliest representative of Herpestidae in the Asian fossil record.

Feliformia indet.

Figure 6D–F

Material: MM-42, left broken P4; stored at the DMR, Bangkok.

Description and comments (fig. 6D–F): The P4 (L = 13.7 mm; W = 5.8 mm) shows a small parastyle and a relatively high paracone (Hpara = 7.5 mm), which is separated from the metastyle by a carnassial notch. A crest extends mesially and slightly buccally from the paracone tip to join the parastyle. Although the mesiolingual part of the tooth is broken (protocone missing), it seems that the tooth is triangular, with a development of the protocone mesial to the paracone tip and close to the parastyle. A crest runs distolingually from the parastyle in the direction of the original location of the protocone. The cingulum is well marked lingually to the metastyle and buccally to the parastyle.

The presence of a carnassial notch, a distinct parastyle, a long metastyle, a poorly developed lingual region, and sharp cusps suggest that this tooth fragment belongs in Feliformia. This specimen appears morphologically closer to the upper carnassial of some viverrids (e.g., *Viverra*, *Viverricula*), prionodontids (extant *Prionodon* species), and felids. The tooth could correspond in size to the lower dental material of cf. *Viverra* sp. from Mae Moh. However, we prefer to maintain the attribution of Feliformia indet. until a more complete upper carnassial is recovered.

PALEOBIOGEOGRAPHY AND PALEOENVIRONMENTS

The Carnivora of Mae Moh brings additional evidence to the hypothesis of a high degree of endemism in northern Thailand during the middle Miocene (Chaimanee et al., 2008). At the generic level, the Mae Moh Basin provides 2 endemic genera (*Maemohcyon*, *Siamictis*). The nonendemic genera are: *Siamogale*, also recorded in the late Miocene and early Pliocene of China; *Vishnuonyx*, for which species are known from the Indian subcontinent and from Kenya during the middle and late Miocene; the Eurasian early to late Miocene *Pseudarctos*; the cosmopolitan Old World taxon *Viverra* (known since the middle Miocene in Asia); and *Leptoplesictis*, recorded in the early and middle Miocene of Europe and Africa, and now for the first time in the middle Miocene of Asia. These occurences suggest faunal dispersals across Southeast Asia, eastern Africa and Europe since at least the middle Miocene. At the specific level, all of the Mae Moh taxa are endemic (except maybe cf. *Pseudarctos* sp. and cf. *Viverra* sp.). The Mae Moh fauna includes numerous other mammals such as rodents, proboscideans, primates, insectivores, cervids, suids, and rhinocerotids (e.g., Ducrocq et al., 1994, 1995; Chaimanee et al., 2007, 2008; Chavasseau et al., 2009; Chaimanee et al., 2011; Suraprasit et al., 2011). Whereas

the large herbivorous mammals generally show affinities with contemporaneous assemblages from the Siwaliks of India and Pakistan and from southern China (Ducrocq et al., 1994), small mammals such as rodents and primates appear morphologically distinct (Chaimanee et al., 2007, 2008). This suggests that northern Thailand may constitute a distinguishable province or subprovince during the middle Miocene, with probably distinctive paleoenvironments (Chaimanee et al., 2008).

The faunal similarity analyses conducted in this study are based on faunal lists that must be viewed with caution because of the need for taxonomic revision of certain localitites, some of which have not been reinvestigated since the first fossil discoveries. Nevertheless, these analyses reveal strong support of paleobiographical patterns that follow the general trends observed for other mammalian groups (e.g., Flynn and Wessels, 2013; Chavasseau et al., 2013; Wang et al., 2019). They reveal three paleobiogeographic provinces for the genera of Carnivora during the middle Miocene: a southern Asian province, clustering together the Pakistani, Indian, and Thai faunas, a Sino-Turkish province, grouping northern Turkish localities of the Sinap Formation with Chinese localities, and a Turkish province with sites from central and southern Turkey (fig. 8A–B, and supplementary appendix S4). The mustelid *Vishnuonyx*, the felid *Vishnufelis*, and the viverrid *Viverra* are exclusive to the southern Asian province during the middle Miocene. During the late Miocene, *Viverra* also occurs in southeastern China (Lufeng). Outside Asia, *Vishnuonyx* is also recorded in the middle Miocene of eastern Africa while *Viverra* is known in the middle and late Miocene in Europe and from the late Miocene to the Pleistocene in Africa.

At the species level, our analyses still suggest the existence of three bioprovinces: a southern Asian one including Indian and Pakistani carnivorans (all Mae Moh species are endemic and therefore are singletons), a Chinese one including carnivorans from the Linxia and Tunggur basins, and a Turkish one (fig. 8C–D, and suppl. appendix S4). In the southern Asian province, most of the species present in Ramnagar (India) are known from the Chinji Formation of the Potwar Plateau (Pakistan): the mustelids *Eomellivora necrophila* and *Vishnuonyx chinjiensis*, the viverrid *Viverra chinjiensis,* and the percrocutid *Percrocuta carnifex*. *Viverra chinjiensis* is also present during the middle Miocene at Chaungtha (Myanmar). The species and genus composition of carnivorans from southern Asia is most dissimilar compared with the Chinese and Turkish faunas (fig. 8A–D, and suppl. appendix S4). During the Miocene, the rapid uplift of the Tibetan Plateau (following the Paleogene Indo-Asian collision) and the retreat of the Paratethys (an epicontinental sea extending over Eurasia during the Paleogene) led to an intensification of the monsoon systems in Asia (Ramstein et al., 1997; Zhang et al., 2007). These events created a strong environmental barrier to terrestrial mammal dispersals between northern and southern Asia (Flynn and Wessels, 2013; Wang et al., 2019). Moreover, some parts of the Himalayan Mountains and the Tibetan Plateau reached their current or near-current elevations during the middle Miocene, preventing north-south faunal exchanges (Deng et al., 2015; Deng and Ding, 2015; Wang et al., 2019).

During the late Miocene, these physical and environmental dispersal barriers were maintained, as carnivoran faunas, based on species composition, are clustered into three assem-

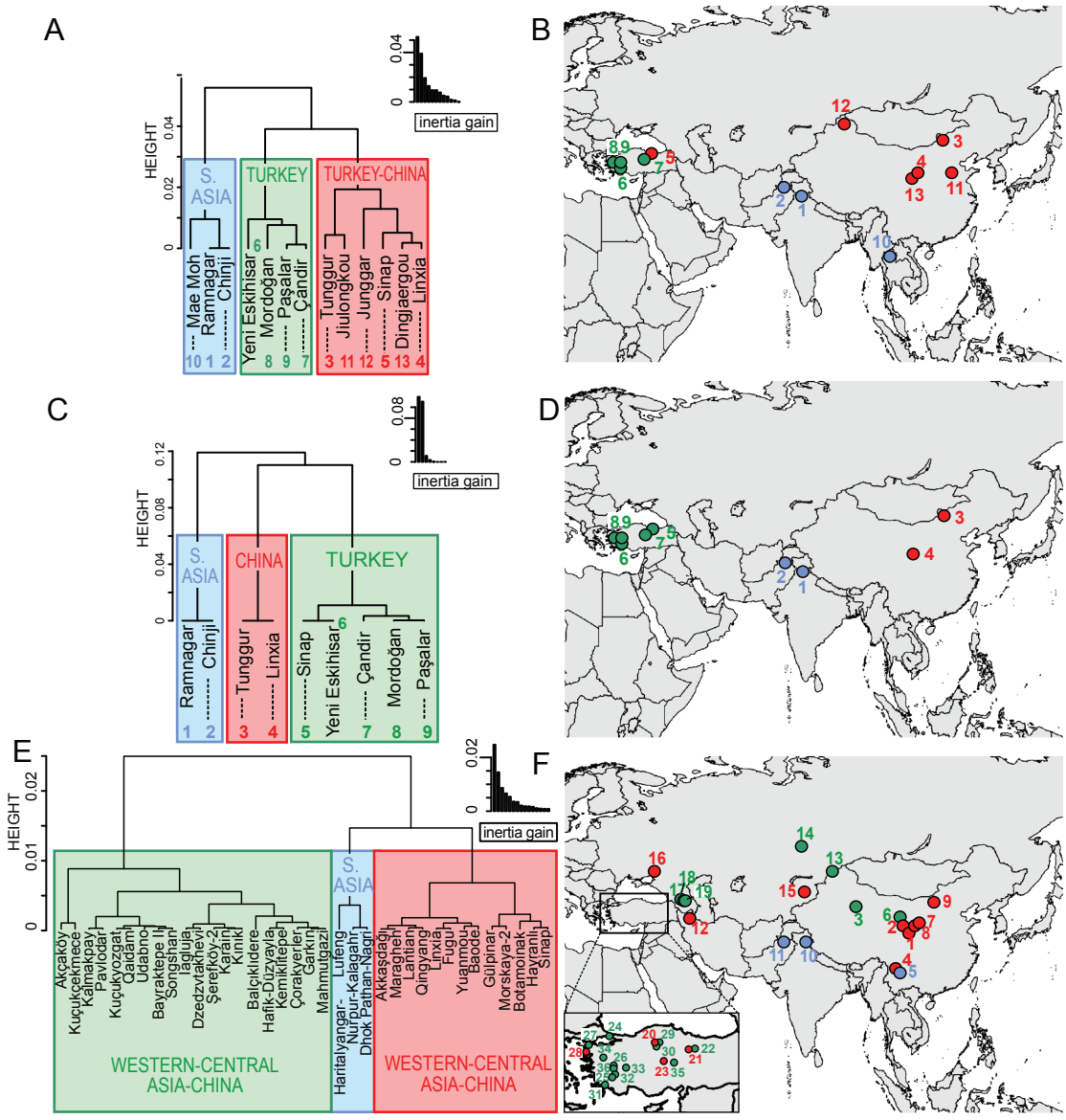

FIGURE 8. UPGMA dendrograms based on NMDS coordinates (**A, C, E**) and associated geographical maps (**B, D, F**) for the middle and late Miocene biogeographical provinces of carnivoran faunas (based on Raup-Crick dissimilarity index). **A–B,** genera of Carnivora from the middle Miocene; **C–D,** species of Carnivora from the middle Miocene; **E–F,** species of Carnivora from the late Miocene. For the middle Miocene (A–D), numbers corresponding to localities are indicated directly in the figure. For the late Miocene (E–F), numbers correspond to the following localities: **1,** Lantian; **2,** Linxia; **3,** Qaidam; **4,** Yuanmou; **5,** Lufeng; **6,** Songshan; **7,** Baode; **8,** Qingyang; **9,** Fugu area; **10,** Haritalyangar-Nurpur-Kalagahr; **11,** Dhok Pathan-Nagri; **12,** Maragheh; **13,** Kalmakpay; **14,** Pavlodar; **15,** Botamoinak; **16,** Morskaya-2; **17,** Dzedzvtakhevi; **18,** Udabno; **19,** Iagluja; **20,** Sinap; **21,** Hayranlı; **22,** Hafik-Düzyayla; **23,** Akkaşdağı; **24,** Kuçukçekmece; **25,** Kemiklitepe; **26,** Akçaköy; **27,** Bayraktepe II; **28,** Gülpinar; **29,** Çorakyerler; **30,** Kuçukyozgat; **31,** Şerefköy 2; **32,** Mahmutgazi; **33,** Garkın; **34,** Kınık; **35,** Karain; **36,** Balçıklıdere.

blages: one regrouping the Siwaliks and Lufeng, and two Asian assemblages regrouping localities from western-central Asia and most of China (except Lufeng; fig. 8E–F, and supplementary appendix S4). Carnivoran species such as *Sivanasua himalayensis*, *Amphicyon palaeindicus*, *Enhydriodon falconneri*, *Viverra chinjiensis*, *Megantereon praecox*, *Lycyaena macrostoma*, *Dinocrocuta gigantea* and *Percrocuta mordax* are recorded both in the Potwar Plateau and the Indian Siwaliks (Haritalyangar-Kalagarh-Nurpur). The otter *Sivaonyx bathygnathus* occurs both in the Dhok Pathan Formation (Potwar Plateau) and Lufeng. However, this species is also known from Yuanmou, the other late Miocene locality from the Yunnan Province. In addition to the presence of *Amphicyon palaeindicus* in Yuanmou, this similarity could have led to the existence a southern Asian biogeographical province including the Siwaliks and southeastern China. However, Yuanmou is clustered in our analysis with other Chinese and central and western Asian localities. We expected a close faunal similarity between Lufeng and Yuanmou, given their close geographic locations and their similar warm and humid climatic conditions influenced by the strengthening of Asian monsoons during the late Miocene (Wang et al., 2019). Perhaps the higher number of carnivoran species in Yuanmou relative to Lufeng (17 and 8 species, respectively), in conjunction with their age difference (7.1–8.5 Ma and 6.2–6.9 Ma, respectively) and the presence of several hyaenas in Yuanmou that are found in Chinese and western Asian localities could explain their dissimilarity in carnivoran assemblages. The fauna of Haritalyangar also comprises the otter *Sivaonyx gandakasensis* that is found in the middle Miocene of Chiang Muan, in Thailand. This occurrence reinforces the hypothesis of a southern Asian province between Southeast Asia and the Siwaliks (Flynn and Wessels, 2013; Chavasseau et al., 2013).

Finally, we failed to find any coherent biogeographical provinces explaining the geographic distributions of carnivoran genera during the late Miocene (suppl. appendix S4). The viverrid *Vishnuictis* and the otter *Enhydriodon* are only recorded in the Siwaliks and in Africa (although ?*Enhydriodon* sp. is reported in Russia). The fauna from Chaingzauk, in Myanmar, does not record any species from the Siwaliks, but includes the cosmopolitan *Ictitherium, Hyaenictitherium*, and *Agriotherium*.

The carnivoran fauna of Mae Moh Basin, mainly represented by semiaquatic mustelids, viverrids, and one herpestid, could support the hypothesis of a mixed tropical and midlatitude deciduous forest constituted by peat swamps or ephemere lakes (Sepulchre et al., 2010; fig. 9). Currently, viverrids are well represented in Southeast Asia with 11, possibly 12 terrestrial civets and arboreal palm civets (Kanchanasakha et al., 1998). They are mainly solitary, nocturnal, and omnivorous forms inhabiting dense tropical forests where they can easily hide on the ground. Some species are known to forage for prey near streams (e.g., *Hemigalus derbyanus*), or to hunt aquatic items in swampy waters (*Cynogale bennettii* and possibly *C. lowei*). Herpestids, occuring mainly in Africa, are known by three extant species in Southeast Asia, including the crab-eating mongoose (*Herpestes urva*) and the poorly known *H. brachyrus*, thought to live in swamps although it is probably a terrestrial hunter. The amphicyonids, less dependent on aquatic environment, are also the scarcest component among the Mae Moh Carnivora fossils.

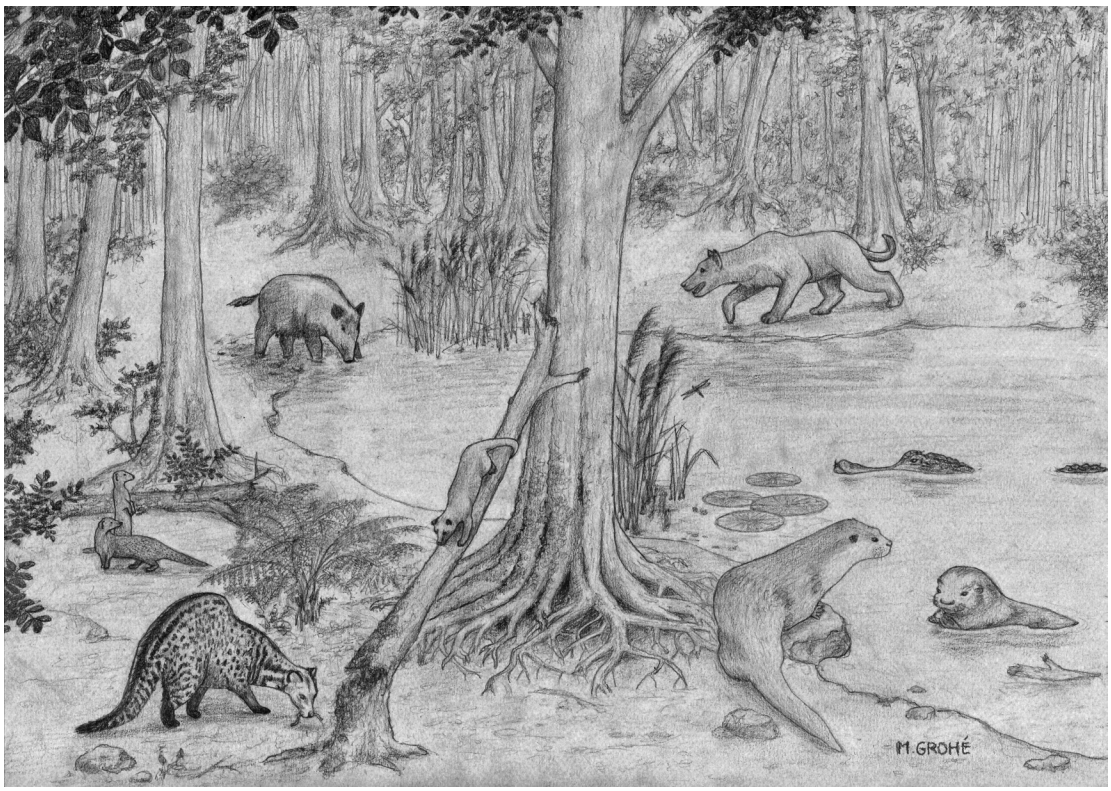

FIGURE 9. A middle Miocene scene in Mae Moh, northern Thailand, illustrating five carnivorans: in the right background *Maemohcyon*, and in the foreground, from right to left, *Siamogale*, *Siamictis*, *Viverra*, and *Leptoplesictis*. Pencil drawing by Mélanie Grohé.

CONCLUSIONS

Nine species of Carnivora are now recorded from the Mae Moh Basin. This fauna appears endemic at the species level. It includes two semiaquatic mustelid genera: the piscivorous otter *Vishnuonyx* and the bunodont otter *Siamogale*, represented by two species and the remains of which are the most abundant among Mae Moh Carnivora. It is worth mentioning that *Vishnuonyx maemohensis* fossils provide the first undoubted record of the lower dentition of the genus and is the most completely known species of this genus. In addition, four smaller feliforms are also present at Mae Moh: two viverrids (including one new genus of Asian palm civet, *Siamictis*), one herpestid (*Leptoplesictis*, which represents the oldest Asian member of the family) and a Feliformia indet. Amphicyonids are reported by a very small species (cf. *Pseudarctos* sp.) and by the largest carnivoran mammal of the Mae Moh community (*Maemohcyon potisati*).

By conducting paleobiogeographical cluster analyses based on middle and late Miocene carnivorans, we highlight the existence of a southern Asian biogeographic province, analogous to the current Oriental Realm, since at the least the middle Miocene. This province results from the physical barrier created by the Himayan Mountains and Tibetan Plateau as well as the

climatic changes they generated through the strengthening of the monsoon systems in Asia. Our study also demonstrates that carnivoran taxa can be used for the reconstruction of biogeographical provinces, and therefore should be integrated in future analyses.

ACKNOWLEDGMENTS

This work has been supported by the Department of Mineral Resources of Bangkok, the Thai-French TRF-CNRS "Cenozoic Biodiversity" Project, the CNRS-*Eclipse* II Program, the ANR-05-BLAN-0235, the ANR-09-BLAN-0238-02-EVAH, the UMR 7262 (PALEVOPRIM, CNRS and University of Poitiers, France), and the Fondation Fyssen (grant to O.C). We would like to thank the Electricity Generating Authority of Thailand for providing scientific assistance and access to the mine. We thank Xavier Valentin and Arnaud Mazurier for their technical support, Sabine Riffaut for her nice drawings, and Vincent Lazzari for providing access to software and computer for 3D reconstructions. We are grateful to John C. Barry, David Pilbeam, Lawrence J. Flynn (Paleoanthropology Laboratory at Harvard University), David Brinkman (Yale Peabody Museum), John J. Flynn and Ruth O'Leary (American Museum of Natural History, New York), and Christine Argot (Muséum National d'Histoire Naturelle, Paris) for providing access to fossils. We are also grateful to Lars Werdelin for providing photos of fossil otters, viverrids and herpestids that greatly helped our comparisons. We thank Stéphane Peigné and L. Werdelin for their helpful comments on the Mae Moh carnivorans. We thank Manuel J. Salesa and one anonymous reviewer for improving the quality of this manuscript. We dedicate this work to our dear colleague S. Peigné.

REFERENCES

Adrian, B., L. Werdelin, and A. Grossman. 2018. New Miocene Carnivora (Mammalia) from Moruorot and Kalodirr, Kenya. Palaeontologia Electronica 21.1.10A: 1–19.

Barry, J.C. 1983. *Herpestes* (Viverridae, Carnivora) from the Miocene of Pakistan. Journal of Paleontology 57 (1): 150–156.

Basu, P.K. 2004. Siwalik mammals of the Jammu Sub-Himalaya, India: An appraisal of their diversity and habitats. Quaternary International 117: 105–118.

Beaumont, G. de. 1973. Contribution à l'étude des viverridés (Carnivora) du Miocène d'Europe. Archives des Sciences de Genève 26: 285–296.

Benammi, M., et al. 2002. Magnetostratigraphy of the Middle Miocene continental sedimentary sequences of the Mae Moh Basin in northern Thailand: evidence for counterclockwise block rotation. Earth and Planetary Science Letters 204: 373–383.

Bonis, L. de, M. Brunet, E.G. Kordikova, and A.V. Mavrin.1997. Oligocene-Miocene sequence stratigraphy and vertebrate paleontology of western and southern Betpakdala Steppe, South Kazakhstan. *In* J.-P. Aguilar, S. Legendre, and J. Michaux (editors), Actes du Congrès BiochroM'97: 225–240 (Mémoires des Travaux de l'E.P.H.E., Institut de Montpellier, vol. 21). Montpellier: E.P.H.E., Institut de Montpellier.

Brayard, A., G. Escarguel, and H. Bucher. 2007. The biogeography of Early Triassic ammonoid faunas: clusters, gradients, and networks. Geobios 40: 749–765.

Chaimanee, Y., et al. 2003. A Middle Miocene hominoid from Thailand and orangutan origins. Nature 422: 61–65.

Chaimanee, Y., C. Yamee, B. Marandat, and J.-J. Jaeger. 2007. First Middle Miocene rodents from the Mae Moh Basin (Thailand): Biochronological and paleoenvironmental implications. Bulletin of the Carnegie Museum of Natural History 39: 157–163.

Chaimanee, Y., C. Yamee, P. Tian, O. Chavasseau, and J.-J. Jaeger. 2008. First middle Miocene sivaladapid primate from Thailand. Journal of Human Evolution 54 (3): 434–443.

Chaimanee, Y., R. Lebrun, C. Yamee, and J.-J. Jaeger. 2011. A new Middle Miocene tarsier from Thailand and the reconstruction of its orbital morphology using a geometric-morphometric method. Proceedings of the Royal Society B 278: 1956–1963.

Chavasseau, O., et al. 2009. New Proboscideans (Mammalia) fron the middle Miocene of Thailand. Zoological Journal of the Linnean Society 155: 703–721.

Chavasseau, O., et al. 2013. Advances in the biochronology and biostratigraphy of the continental Neogene of Myanmar. *In* X. Wang, L.J. Flynn, and M. Fortelius (editors), Fossil mammals of Asia: Neogene biostratigraphy and chronology: 461–474. New York: Columbia University Press.

Colbert, E.H. 1933. A new mustelid from the Lower Siwalik beds of northern India. American Museum Novitates 605: 1–3.

Colbert, E.H. 1935. Siwalik mammals in the American Museum of Natural History. Transactions of the American Philosophical Society 26: 1–401.

Colbert, E.H. 1939. Carnivora of the Tung Gur Formation of Mongolia. Bulletin of the American Museum of Natural History 76 (2): 47–81.

Corsiri, R., and A. Crouch. 1985. Mae Moh Coal Deposit. Geologic Report: Thailand/Australia Lignite Mines Development Project, Electricity Generating Authority of Thailand 1: 1–448.

Coster, P., et al. 2010. A complete magnetic polarity stratigraphy of the Miocene continental deposits of Mae Moh basin, northern Thailand and a reassessment of the age of hominoid bearing localities in northern Thailand. Geological Society of America Bulletin 122: 1180–1191.

Dehghani, R., and L. Werdelin. 2008. A new small carnivoran from the Middle Miocene of Fort Ternan, Kenya. Neues Jahrbuch für Geologie und Paläontologie, Abhandlungen 248: 233–244.

Deng, T., and L. Ding. 2015. Paleo-altimetry reconstructions of the Tibetan Plateau: progress and contradictions. National Science Review 93: 92–95.

Deng, T., X. Wang, S.-Q. Wang, Q. Li, and S.-K. Hou. 2015. Evolution of the Chinese Neogene mammalian faunas and its relationship to uplift of the Tibetan Plateau. Advances in Earth Science 30: 407–415.

Depéret, C. 1890. Les animaux pliocènes du Rousillon. Mémoire de la Société Géologique de France 3: 1–88.

Dong, W., and G. Qi. 2013. Hominoid-producing localities and biostratigraphy in Yunnan. *In* X. Wang, L.J. Flynn, and M. Fortelius (editors), Fossil mammals of Asia: Neogene biostratigraphy and chronology: 293–313. New York: Columbia University Press.

Ducrocq, S., Y. Chaimanee, V. Suteehorn, and J.-J. Jaeger. 1994. Ages and paleoenvironment of Miocene mammalian faunas from Thailand. Palaeogeography, Palaeoclimatology, Palaeoecology 108: 149–163.

Ducrocq, S., Y. Chaimanee, V. Suteehorn, and J.-J. Jaeger. 1995. Mammalian faunas and the ages of the continental Tertiary fossiliferous localities from Thailand. Journal of Southeast Asian Earth Sciences 12 (1/2): 65–78.

Flynn, L.J., and W. Wessels. 2013. Paleobiogeography and South Asian small mammals. *In* X. Wang, L.J. Flynn, and M. Fortelius (editors), Fossil mammals of Asia: Neogene biostratigraphy and chronology: 444–460. New York: Columbia University Press.

Fraile, S., B. Ferez, I. De Miguel, and J. Morales 1997. Revision de los Carnivoros presentes en los yacimientos del Neogeno espanol. *In* J.P. Calvo and J. Morales (editors), Avances en el conocimiento del Terciario iberico: 77–80 (Tercero congreso del Grupo Español del Terciario, Cuenca (Spain), 2–4 Jul 1997, CSIC). Madrid: Museo Nacional de Ciencias Naturales, Universidad Complutense, Facultad de Ciencias Geologicas.

Gaillard, C. 1899. Mammifères miocènes nouveaux ou peu connus de la Grive-Saint-Alban (Isère). Archives du Muséum d'histoire naturelle de Lyon 7: 1–11.

Geraads, D. 1997. Carnivores du Pliocène terminal d'Ahl al Oughlam (Casablanca, Maroc). Geobios 30: 127–164.

Geraads, D., V. Eisemann, and G. Petter. 2004. The large mammal fauna of the Oldowayan sites of Melka-Kunturé, Ethiopia. *In* J. Chavaillon and M. Piperno (editors), Studies on the early palaeolithic site of Melka Kunturé, Ethiopia: 169–192. Florence: Istituto Italiano di Preistoria e Protoistoria.

Gervais, P. 1967–1969. Zoologie et paléontologie générales: nouvelles recherches sur les animaux vertébrés vivants et fossiles. Paris: A. Bertrand.

Ginsburg, L. 1961. La faune des carnivores miocènes de Sansan (Gers). Mémoires du Muséum national d'Histoire naturelle (sér. C) 9: 1–190.

Ginsburg, L. 1992. Les genres *Pseudarctos* et *Ictiocyon*, Amphicyonidae (Carnivora, Mammalia) du Miocène européen. Bulletin du Muséum National d'Histoire Naturelle 4 (14): 301–317.

Ginsburg, L. 2002. Les carnivores fossiles des sables de l'Orléanais. Annales de Paléontologie 88 (2): 115–146.

Ginsburg, L., and P. Tassy. 1985. The fossil mammals and the age of the lignite beds in the intramontane basins of northern Thailand. Journal of the Geological Society of Thailand 8: 13–27.

Ginsburg, L., and M. Telles Antunes. 1968. *Amphicyon giganteus* Carnassier géant du Miocène. Annales de Paléontologie 54 (1): 1–32.

Ginsburg, L., and J.-L. Welcomme. 2002. Nouveaux restes de créodontes et de carnivores des Bugti (Pakistan). Symbioses 7: 65–68.

Ginsburg, L., R. Ingavat, and P. Tassy. 1983. *Siamogale thailandica*, nouveau Mustelidae (Carnivora, Mammalia) néogène du Sud-Est asiatique. Bulletin de la Société Géologique de France 25 (6): 953–956.

Gradstein, F.M., J.G. Ogg, M.D. Schmitz, and G.M. Ogg. 2012. The Geological Time Scale 2012. Elsevier: Amsterdam.

Grohé, C., et al. 2010. New data on Mustelidae (Carnivora) from Southeast Asia: *Siamogale thailandica*, a peculiar otter-like mustelid from the late Middle Miocene Mae Moh Basin, northern Thailand. Naturwissenschaften 97: 1003–1015.

Grohé, C., Y. Chaimanee, C. Blondel, and J.-J. Jaeger. 2012. Carnivora from the Miocene of southern Asia and Africa: biogeographical implications. Terra Nostra (Centenary Meeting of the Paläontologische Gesellschaft, Berlin) 3 (S20): 65.

Grohé, C., L. de Bonis, Y. Chaimanee, C. Blondel, and J.-J. Jaeger. 2013. The oldest Asian *Sivaonyx* (Lutrinae, Mustelidae): a contribution to the evolutionary history of bunodont otters. Palaeontologia Electronica 16.3.29A: 1–13.

Grohé, C., L. de Bonis, Y. Chaimanee, J. Surault, and J.-J. Jaeger. 2020. 3D models related to the publication: The late middle Miocene Mae Moh Basin of northern Thailand: the richest Neogene fauna of Carnivora from Southeast Asia and a paleobiogeographic analysis of Miocene eastern Asian faunas. MorphoMuseuM 6: e109. [doi: 10.18563/journal.m3.109]

Haile-Selassie, Y. 2008. New observations on the Late Miocene-Early Pliocene Lutrinae (Mustelidae: Carnivora, Mammalia) from the Middle Awash, Afar Rift, Ethiopia. Comptes Rendus Palevol 7: 55–569.

Hendey, Q.B. 1974. The Late Cenozoic Carnivora of the southwestern Cape Province. Annals of the South African Museum 63: 1–369.

Howell, F.C. 1987. Preliminary observations on Carnivora from the Sahabi Formation (Libya). *In* N.T. Boaz, A. El-Arnauti, A.W. Gaziry, J. de Heinzelin, and D.D. Boaz (editors), Neogene paleontology and geology of Sahabi: 153–181. New York: A.R. Liss.

Hunt, R.M., Jr. 2003. Intercontinental migration of large mammalian carnivores: earliest occurence of the Old World beardog *Amphicyon* (Carnivora, Amphicyonidae) in North America. *In* Lawrence J. Flynn (editor), Vertebrate fossils and their context: contributions in honor of Richard H. Tedford, chapter 4. Bulletin of the American Museum of Natural History 279: 77–115.

Jiangzuo Q., C. Li, X. Zhang, S. Wang, J. Ye, and Y. Li. 2018. Diversity of Amphicyonidae (Carnivora, Mammalia) in the Middle Miocene Halamagai formation in Ulungur River area, Xinjiang, northwestern China. Historical Biology. [doi:10.1080/08912963.2018.1477142]

Jiangzuo Q., C. Li, S. Wang, and D. Sun. 2019. *Amphicyon zhanxiangi*, sp. nov., a new amphicyonid (Mammalia, Carnivora) from northern China. Journal of Vertebrate Paleontology. [doi:10.1080/02724634.2018.1539857]

Kanchanasakha, B., S. Simcharoen, and U.T. Than. 1998. Carnivores of mainland South East Asia. Bangkok: WWF-Thailand.

Koenigswald, G.R.D. von. 1959. A mastodont and other fossil mammals from Thailand. Report of Investigation of Royal Department of Mines 2: 25–28.

Kohno, N. 1997. The first record of an amphicyonid (Mammalia: Carnivora) from Japan, and its implication for amphicyonid paleobiogeography. Paleontological Research 1 (4): 311–315.

Kordikova, E.G. 2001. Remarks on the Oligocene-Miocene mammal paleontology and sequence stratigraphy of south-western Betpakdala Steppe, South Kazakhstan. Neues Jahrbuch für Geologie und Palaontologie Abhandlungen 221 (1): 35–79.

Kreft, H., and W. Jetz. 2010. A framework for delineating biogeographical regions based on species distributions. Journal of Biogeography 37: 2029–2053.

Lydekker, R. 1876. Molar teeth and other remains of Mammalia. Memoirs of the Geological Survey of India, Palaeontologia Indica (ser. 10) 1: 19–87.

Lydekker, R. 1884. Indian Tertiary and post-Tertiary Vertebrata, vol. 2, pt. 6: Siwalik and Narbada Carnivora. Memoirs of the Geological Survey of India, Palaeontologia Indica 10: 178–355.

Major, C.I.F. 1903. New Carnivora from the Middle Miocene of La Grive-Saint-Alban, Isère, France. Geological Magazine 10: 534–538.

Matthew, W.D. 1929. Critical observations upon Siwalik mammals. Bulletin of the American Museum of Natural History 56 (7): 437–560.

Mein, P., and L. Ginsburg. 1997. Les mammifères du gisement miocène inférieur de Li Mae Long, Thaïlande : systématique, biostratigraphie et paléoenvironnement. Geodiversitas 19: 783–844.

Métais, G., et al. 2009. Lithofacies, depositional environments, regional biostratigraphy and age of the Chitarwata Formation in the Bugti Hills, Balochistan, Pakistan. Journal of Asian Earth Sciences 34: 154–167.

Morales, J., and M. Pickford. 2005. Carnivores from the middle Miocene Ngorora Formation (13–12 Ma), Kenya. Estudios Geologicos 61: 271–284.

Morales, J., and M. Pickford. 2008. Creodonts and carnivores from the Middle Miocene Muruyur Formation at Kipsaraman and Cheparawa, Baringo district, Kenya. Comptes Rendus Palevol 7: 487–497.

Morales, J., and M. Pickford. 2011. A new paradoxurine from the Late Miocene Siwaliks of India and a review of the bunodont viverrids of Africa. Geobios 44: 271–277.

Morales, J., M. Nieto, M. Kohler, and S. Moyà-Solà. 1999. Large mammals from the Vallesian of Spain. *In* J. Agusti, L. Rook, and P. Andrews (editors), Hominoid evolution and climatic change in Europe, vol. 1. The evolution of Neogene terrestrial ecosystems in Europe: 113–126. Cambridge: Cambridge University Press.

Morales, J., M. Pickford, D. Soria, and S. Fraile 2001. New Viverrinae (Carnivora: Mammalia) from the basal Middle Miocene of Arrisdrift, Namibia. Palaeontologica Africana 37: 99–102.

Morales, J., D. Soria, and M. Pickford. 2005. Carnivores from the Late Miocene and basal Pliocene of the Tugen Hills, Kenya. Revista de la Sociedad Geológica de España 18 (1–2): 39–61.

Morales, J., M. Pickford, and M.J. Salesa. 2008. Creodonta and Carnivora from the early Miocene of the northern Sperrgebiet, Namibia. Memoir of the Geological Survey of Namibia 20: 291–310.

Morlo, M., E.R. Miller, and A. El-Barkooky. 2007. Creodonta and Carnivora from Wadi Moghra, Egypt. Journal of Vertebrate Paleontology 27: 145–159.

Nanda, A.C., and R.K. Sehgal. 1993. Siwalik mammalian faunas from Ramnagar (J. & K.) and Nurpur (H.P.) and lower limit of *Hipparion*. Journal of Geological Society of India 42: 115–134.

Patnaik, R. 2013. Indian Neogene Siwalik mammalian biostratigrahy, an overview. *In* X. Wang, L.J. Flynn, and M. Fortelius (editors), Fossil mammals of Asia: Neogene biostratigraphy and chronology: 423–444. New York: Columbia University Press.

Peigné, S. 2013. Les Carnivora de Sansan. *In* S. Peigné and S. Sen (editors), Mammifères de Sansan: 559–660 (Mémoires du Muséum National d'Histoire Naturelle 203). Paris: Muséum d'Histoire Naturelle.

Peigné, S., Y. Chaimanee, C. Yamee, P. Tian, and J.-J. Jaeger. 2006. A new amphicyonid (Mammalia, Carnivora, Amphicyonidae) from the late Miocene of northern Thailand and a review of the amphicyonine record in Asia. Journal of Asian Earth Sciences 26: 519–532.

Peigné, S., et al. 2008. Late Miocene Carnivora from Chad: Herpestidae, Viverridae and small-sized Felidae. Comptes Rendus Palevol 7 (8): 499–527.

Petter, G. 1963. Étude de quelques viverridés (Mammifères, Carnivores) du Pléistocène inférieur du Tanganyika (Afrique orientale). Bulletin de la Société Géologique de France (ser. 5) 7: 265–274.

Petter, G. 1967. Petits carnivores villafranchiens du Bed I d'Oldoway (Tanzanie). Problèmes actuels de Paléontologie (Evolution des Vertébrés), Colloques Internationaux du Centre National de la Recherche Scientifique (CNRS) Paris 163: 529–538.

Petter, G. 1973. Carnivores pléistocènes du ravin d'Olduvai, Tanzanie. Fossil vertebrates of Africa 3: 43–100.

Petter, G. 1987. Small carnivores (Viverridae, Mustelidae, Canidae) from Laetoli. *In* M.D. Leakey and J.M. Harris (editors), Laetoli, a Pliocene site in northern Tanzania: 194–234. Oxford: Clarendon Press.

Petter, G., and F.C. Howell. 1977. Diversification des civettes (Carnivora, Viverridae) dans les gisements pléistocènes de l'Omo. Comptes Rendus de l'Académie des Sciences de Paris 284: 283–286.

Petter, G., M. Pickford, and F.C. Howell. 1991. La loutre piscivore du Pliocène de Nyaburogo et de Nkondo (Ouganda, Afrique orientale): *Torolutra ougandensis* n.g., n.sp. (Mammalia, Carnivora). Comptes Rendus de l'Académie des Sciences 312: 949–955.

Pickford, M. 2007. Revision of the Mio-Pliocene bunodont otter-like mammals of the Indian Subcontinent. Estudios geologicos 63 (1): 83–127.

Pilbeam, D.R., A.K. Behrensmeyer, J.C. Barry, and S.M. Ibrahim Shah. 1979. Miocene Sediments and Faunas of Pakistan. Postilla 179: 1–45.

Pilgrim, G.E. 1910. Notices of new mammalian genera and species from the Tertiaries of India. Records of the Geological Survey of India 40: 63–71.

Pilgrim, G.E. 1912. The vertebrate fauna of the Gaj Series in the Bugti Hills and the Punjab. Memoirs of the Geological Survey of India, Palaeontologia Indica 4: 1–83.

Pilgrim, G.E. 1932. The fossil Carnivora of India. Memoirs of the Geological Survey of India. Palaeontologia Indica 18: 1–232.

Prasad, K.N. 1968. The vertebrate fauna from the Siwalik beds of Haritalyangar, Himachal Pradesh, India. Memoirs of the Geological Survey of India. Paleontologia Indica 39: 1–79.

Qi, G. 2004. *Lufengictis*, a new genus of viverrids from *Lufengpithecus* locality of Yunnan. Acta Anthropologica Sinica 23: 277–285.

Qi, G. 2006. Carnivora. *In* G. Qi, and W. Dong (editors), *Lufengpithecus hudiensis* Site: 149–177. Beijing: Science Press.

Qi, G., et al. 2006. Taxonomy, age and environment status of the Yuanmou hominoids. Chinese Science Bulletin 51 (6): 704–712.

Qi, T. 1989. Miocene Carnivores from Altai Region, Xinjiang. Vertebrata PalAsiatica 27: 133–139.

Qiu, Z. 1980. *Viverra peii*, a new species from the "Cap" travertine of Zhoukoudien. Vertebrata PalAsiatica 18: 304–313.

Qiu, Z., D. Yan, H. Jia, and B. Sun. 1986. The large-sized ursid fossils from Shanwang, Shandong. Vertebrata PalAsiatica 24: 182–194.

Qiu, Z.d., and Z.x. Qiu. 2013. Early Miocene Xiejiahe and Sihong fossil localities and their faunas, eastern China. *In* X. Wang, L.J. Flynn, and M. Fortelius (editors), Fossil mammals of Asia: Neogene biostratigraphy and chronology: 142–154. New York: Columbia University Press.

Ramstein, G., F. Fluteau, J. Besse, and S. Joussaume. 1997. Effect of orogeny, plate motion and land-sea distribution on Eurasian climate change over the past 30 million years. Nature 386: 788–795.

Raza, S.M., J.C. Barry, G.E. Mayer, and L. Matin. 1984. Preliminary report on the geology and vertebrate fauna of the Miocene Manchar formation, Sind, Pakistan. Journal of Vertebrate Palaeontology 4: 584–599.

Roth, C. 1988. *Leptoplesictis* Major 1903 (Mammalia, Carnivora, Viverridae) aus dem Orleanium und Astaracium/Miozän von Frankreich und Deutschland. Paläontologische Zeitschrift 62: 333–343.

Rook, L., and B. Martinez-Navarro. 2004. *Viverra howelli* n. sp., a new viverrid (Carnivora, Mammalia) from the Baccinello-Cinigiano Basin (Latest Miocene, Italy). Rivista Italiana di Paleontologia e Stratigrafia 110: 719–723.

Savage, R.J.G. 1965. The Miocene Carnivora of East Asia. Fossil Mammals of Africa, 19. Bulletin of the British Museum (Natural History), Geology 70 (8): 242–312.

Schlosser, M. 1888. Die Affen, Lemuren, Chiropteren, Insectivoren, Marsupialier, Creodonten und Carnivoren des Europäischen Tertiärs. Teil 2. Beiträge zur Paläontologie Osterreich-Ungarns 7: 1–162.

Schlosser, M. 1899. Über die Bären und bärenähnlichen Formen des europäischen Tertiärs. Palaeontographica 46: 95–148.

Schmidt-Kittler, N. 1987. The Carnivora (Fissipeda) from the lower Miocene of East Africa. Palaeontographica A 197: 85–126.

Sein, C., and T. Thein. 2011. A New Amphicyonid (Mammalia, Carnivora) from the Ayeyarwady Formation of Central Myanmar. Universities Research Journal 4 (5): 47–57.

Sepulchre, P., D. Jolly, Y. Chaimanee, J.-J. Jaeger, and A. Raillard. 2010. Mid-Tertiary paleoenvironments in Thailand: pollen evidence. Climate of the Past 6: 461–473.

Songtham, W., et al. 2005, Middle Miocene Molluscan assemblages in Mae Moh basin, Lampang Province, northern Thailand. ScienceAsia 31: 183–191.

Stehlin, H.G., and H. Helbing. 1925. Catalogue des ossements de mammifères tertiaires de la collection Bourgeois à l'Ecole de Pont-Levoy (Loir-et-Cher). Bulletin de la Société d'Histoire Naturelle et d'Anthropologie de Loir-et-Cher 18: 77–277.

Suraprasit, K., Y. Chaimanee, T. Martin, and J.-J. Jaeger. 2011. First Castorid (Mammalia, Rodentia) from the Middle Miocene of Southeast Asia. Naturwissenschaften 98: 315–328.

Suraprasit, K., Y. Chaimanee, H. Bocherens, O. Chavasseau, and J.-J. Jaeger. 2014. Systematics and phylogeny of Middle Miocene Cervidae (Mammalia) from Mae Moh Basin (Thailand) and a palaeoenvironmental estimate using enamel isotopy of sympatric herbivore species. Journal of Vertebrate Paleontology 34: 179–194.

Suraprasit, K., Y. Chaimanee, O. Chavasseau, and J.-J. Jaeger. 2015. Middle Miocene bovids from Mae Moh Basin, northern Thailand: The first record of the genus *Eotragus* from Southeast Asia. Acta Palaeontologica Polonica 60 (1): 67–78.

Takai, M., H. Saegusa, Thaung-Htike, and Zin-Maung-Maung-Thein. 2006. Neogene mammalian fauna in Myanmar. Asian Paleoprimatology 4: 143–172.

Tassy, P., P. Anupandhanant, L. Ginsburg, P. Mein, and B. Ratanasthien. 1992. A new *Stegolophodon* (Proboscidea, Mammalia) from the early Miocene of northern Thailand. Geobios 25: 511–523.

Teilhard de Chardin, P., and P. Leroy. 1945. Les mustélidés de Chine. Publications de l'Institut de Géobiologie 12: 1–56.

Tiwari, B.N. 1983. Lower Siwalik faunas of the Indian subcontinent with special reference to Kalagarh Fauna. Publications of the Centre of Advanced Study in Geology (Panjab University, Chandigarh) 13: 98–112.

Tseng, Z.J., J.K. O'Connor, X. Wang, and D.R. Prothero. 2009. The first Old World occurrence of the North American mustelid *Sthenictis* (Mammalia, Carnivora). Geodiversitas 31 (4): 743–751.

Valenciano, A., et al. 2019. First record of *Hoplictis* (Carnivora, Mustelidae) in East Asia from the Miocene of the Ulungur river area, Xinjiang, northwest China. Acta Geologica Sinica 93 (2): 251–264.

Wang, S.-Q., et al. 2019. Yunnan, a refuge for trilophodont proboscideans during the late Miocene aridification of East Asia. Palaeogeography, Palaeoclimatology, Palaeoecology 515: 162–171.

Wang, X. 2004. New materials of *Tungurictis* (Hyaenidae, Carnivora) from Tunggur Formation, Nei Mongol. Vertebrata PalAsiatica 42: 144–153.

Wang, X., et al. 1998. Carnivora from middle Miocene of northern Junggar Basin, Xinjiang autonomous region, China. Vertebrata PalAsiatica 36: 218–243.

Wang, X., Z. Qiu, and N.D. Opdyke. 2003. Litho-, Bio- and Magnetostratigraphy and Paleoenvironment of Tunggur Formation (Middle Miocene) in Central Inner Mongolia, China. American Museum Novitates 3411: 1–31.

Wang, X., Z. Qiu, and B.-Y. Wang. 2005. Hyaenodonts and carnivorans from the early Oligocene to early Miocene of Xianshuihe formation, Lanzhou basin, Gansu Province, China. Palaeontologia Electronica 8.1.6: 1–14.

Wang, X., et al. 2018. A new otter of giant size, *Siamogale melilutra* sp. nov. (Lutrinae: Mustelidae: Carnivora), from the latest Miocene Shuitangba site in north-eastern Yunnan, south-western China, and a total-evidence phylogeny of lutrines. Journal of Systematic Palaeontology 16: 39–65.

Wang, X., et al. 2020. A new species of *Tungurictis* (Carnivora, Hyaenidae) from the middle Miocene of Junggar Basin, northwestern China and early divergence of basal hyaenids in East Asia. Geodiversitas 42 (3): 29–45.

Werdelin, L., 2003. Mio-Pliocene Carnivora from Lothagam, Kenya. *In* M.G. Leakey and J.M. Harris (editors), The dawn of humanity in eastern Africa: 261–328. New York: Columbia University Press.

Werdelin, L. 2019. Middle Miocene Carnivora and Hyaenodonta from Fort Ternan, western Kenya. *In* L. de Bonis and L. Werdelin (editors), Memorial to Stéphane Peigné: carnivores (Hyaenodonta and Carnivora) of the Cenozoic. Geodiversitas 41 (6): 267–283.

Werdelin, L., and M.E. Lewis. 2013. Koobi Fora research project, vol. 7. The Carnivora. San Francisco: California Academy of Sciences.

Werdelin, L., and S. Peigné. 2010. Carnivora. *In* L. Werdelin and W.J. Sanders (editors), Cenozoic mammals of Africa: 609–663. Berkeley: University of California Press.

West, R.M., J.R. Lukacs, J.J. Munthe, and S.T. Hussain. 1978. Vertebrate fauna from Neogene Siwalik Group, Dang Valley, western Nepal. Journal of Paleontology 52 (5): 1015–1022.

Zhang, Z.-S., H.-J. Wang, Z.-T. Guo, and D.-B. Jiang. 2007. What triggers the transition of palaeoenvironmental patterns in China, the Tibetan Plateau uplift or the Paratethys Sea retreat? Palaeogeography, Palaeoclimatology, Palaeoecology 245: 317–331.

All issues of *Novitates* and *Bulletin* are available on the web (http://digitallibrary.amnh.org/dspace). Order printed copies on the web from:
http://shop.amnh.org/a701/shop-by-category/books/scientific-publications.html

or via standard mail from:

American Museum of Natural History—Scientific Publications
Central Park West at 79th Street
New York, NY 10024

♾ This paper meets the requirements of ANSI/NISO Z39.48-1992 (permanence of paper).